Electronic Research Archive

https://www.aimspress.com/journal/era

ERA, 34(6): 3858–3894.
DOI: 10.3934/era.2026174
Received: 08 March 2026
Revised: 17 April 2026
Accepted: 24 April 2026
Published: 12 May 2026

Research article

Qualitative analysis and numerical simulation of pattern evolution in a vegetation-water model incorporating saturated water absorption and intraspecific competition

Xiaozhou Feng*, Tingting Li, Changtong Li*, Dongping Li and Hua Shi

School of Science, Xi'an Technological University, Xi'an 710032, China

* **Correspondence:** Email: flxzfxz8@163.com, lctnihao@163.com.

Abstract: In this paper, we propose a vegetation-water coupled system that explicitly incorporates saturated water absorption and an intraspecific competition term. We first establish the global stability of the boundary equilibrium, then analyze the stability and Turing instability of the positive equilibria, demonstrating that the equilibrium with low vegetation density is consistently unstable, while the other positive equilibrium exhibits Turing instability when the vegetation diffusion coefficient is sufficiently small or the water diffusion coefficient is sufficiently large. We derive a priori estimates for nonnegative steady-state solutions via the maximum principle, conduct a detailed qualitative analysis of steady-state bifurcations at simple and double eigenvalues, and establish criteria for the bifurcation direction. Finally, through numerical simulations, we present the dynamical behaviors near the bifurcation points and simulate the evolution of vegetation patterns under different parameter settings, and find that as the water diffusion coefficient d_1 and the intraspecific competition coefficient σ increase, Turing patterns transition from spot-like to stripe-like structures; conversely, as the precipitation parameter a increases, the patterns shift from stripe-like to spot-like. These findings advance our understanding of the mechanisms governing vegetation pattern formation in water-limited ecosystems and provide a theoretical framework for predicting ecosystem responses to environmental changes.

Keywords: vegetation-water system; turing instability; global stability; steady-state bifurcation; intraspecific competition

1. Introduction

Desertification [1], a pervasive global ecological crisis, has been continuously expanding in arid and semi-arid regions [2]. Even some semi-humid gully areas have shown signs of deterioration. The core of this issue lies in the combined effects of climate change [3, 4], alterations in soil properties, and vegetation cover degradation, which ultimately leads to a progressive decline in essential

ecosystem services. Desertification has accelerated markedly under the dual pressures of changing natural conditions [5, 6] and anthropogenic disturbances [7–9]. This acceleration disrupts vegetation structure and function, leading to the decline of dominant species, community simplification, and, ultimately, vegetation degradation [10, 11] and reduced coverage. Therefore, promoting the scientific restoration and sustainable long-term management of vegetation ecosystems has become an urgent priority in addressing the challenge of desertification [12].

Intraspecific competition [13] also profoundly influences vegetation dynamics. Different plant species compete for resources such as light, water, and nutrients, leading to an increase in dominant species and a decline in inferior ones. Consequently, investigating the dynamic evolution mechanisms of vegetation-water systems has emerged as a pivotal research direction in ecological theory, holding key significance for mitigating ecological crises and achieving a balance between ecological conservation and development.

For decades, many scholars have proposed relevant mathematical systems to study desertification. For example, Donzelli et al. [14] established a vegetation-water system in arid and sparsely wooded grassland areas and discussed the steady-state and bifurcation analysis of the system; considering the differences in root depths of different vegetation leading to different water absorption capacities, Ying et al. [15] constructed a vegetation-water system and analyzed the stability of equilibrium points. However, the above studies did not consider the spatial diffusion phenomenon in ecosystems. For this reason, many scholars have introduced spatial diffusion into vegetation-water systems, constructing them with partial differential equations to further explore their dynamic behaviors. From 1997 to 2008, Lefever et al. [16, 17] established a spatial diffusion system that contained unique vegetation, explored the causes of irregular patterns, and discussed the system's dimensionless results:

$$\frac{\partial n}{\partial t} = (1-\mu)n + (\Lambda-1)n^2 - n^3 + \frac{1}{2}(L^2-n)\Delta n - \frac{1}{8}n\Delta n. \tag{1.1}$$

This model mainly explores the pattern change of a single plant species and does not consider the synergistic interactions of water and vegetation.

In desertification research, water is a core factor affecting vegetation growth and land degradation processes, and its role is crucial. Klausmeier [18] constructed a vegetation-water system with spatial diffusion and studied its Turing instability.

$$\begin{cases} \dfrac{\partial W}{\partial T} = A - LW - RWN^2 + V\dfrac{\partial W}{\partial X}, \\ \dfrac{\partial N}{\partial T} = RJWN^2 - MN + D\Delta N. \end{cases} \tag{1.2}$$

This model effectively captures the coupling mechanisms among precipitation, evaporation, runoff, and vegetation water uptake, as well as the resulting spatial self-organized patterns, providing a solid ecohydrological basis. However, under sufficient water availability, its biomass exhibits unbounded growth, failing to reflect density dependence, and the threshold processes of ecosystem recovery following degradation.

Subsequently, extensive research has been conducted on the spatial distribution patterns of vegetation, leading to the development of various systems. For instance, studies based on the Rietkerk system and modified versions of both the Klausmeier and Rietkerk systems [19] have explored the mechanisms underlying real-world vegetation patterns and the influence of natural factors. Vegetation

water absorption is a vital physiological process in vegetation growth. With vegetation biomass increases to a certain extent, vegetation reach water absorption saturation. The saturation effect of vegetation water absorption was considered by Li et al. [20], and the saturated water absorption rate of vegetation was expressed as $\frac{aN}{1+bN}$, and a system with water absorption saturation effect was proposed.

$$\begin{cases} \dfrac{\partial W}{\partial T} = A - LW - RW\dfrac{aN^2}{1+bN} + D_1\Delta W, \\ \dfrac{\partial N}{\partial T} = RJW\dfrac{aN^2}{1+bN} - MN + D_2\Delta N. \end{cases} \tag{1.3}$$

In recent years, numerous scholars have conducted extensive research on the dynamical mechanisms of vegetation-water coupled systems and have achieved fruitful results. Li et al. [21] developed a vegetation-water model incorporating the effect of hydrotropism, revealing that hydrotropism can also promote the growth of vegetation itself. Zhang and Wu [22] focused on a vegetation-water model with cross-diffusion, and using Floquet theory, derived conditions under which stable periodic solutions become unstable. Xiong et al. [23] established a cross-diffusion model with mixed delays to describe vegetation dynamics under water shortage conditions. Guo et al. [24] studied a vegetation-water model with saturated water absorption and found that the equilibrium with low vegetation density is always unstable. Furthermore, Wang and Zhang [25] extended the Klausmeier system and deeply explored the influence mechanism of internal biological competition on the formation of vegetation spatial patterns:

$$\begin{cases} \dfrac{\partial v}{\partial t} = p - w - \dfrac{wn^2}{1+\sigma^* n^2} - v\dfrac{\partial v}{\partial x}, & x \in \Omega, t > 0, \\ \dfrac{\partial n}{\partial t} = \dfrac{wn^2}{1+\sigma^* n^2} - \delta n + \nabla^2 n, & x \in \Omega, t > 0. \end{cases} \tag{1.4}$$

The numerator of $\frac{wn^2}{1+\sigma^* n^2}$ reflects the long-range competition and short-range promotion, and the denominator represents the internal or local competition among organisms. The parameter σ represents the intensity of internal competition response. If the negative feedback caused by internal competition is stronger than the positive feedback caused by infiltration, the available water of individual plants may decrease.

In the study of arid vegetation-water coupled models, the mathematical formulation of competitive terms is not a unique standard form, and multiple reasonable modeling frameworks have been developed in the academic community. For example, to investigate the effects of intraspecific competition on species coexistence in banded vegetation, Eigentler [26] incorporated logistic-type density-dependent competitive terms into the growth rates of plant species in a multispecies model, embedding the logistic constraint of the form $(1 - u/k)$ to characterize the regulatory effect of intraspecific competition on vegetation growth. The generalized Holling type-III functional response is a classical mathematical framework for characterizing nonlinear saturated responses in population dynamics, featuring linear response at low intensity and quadratic saturation at high intensity, which is widely applicable to dynamic modeling of various ecosystems. Dai et al. [27] introduced the generalized Holling type-III functional response into the ecological dynamic system. Motivated by this classical modeling approach, this paper extends the mathematical mechanism of the generalized Holling type-III functional response to the vegetation-water coupled system.

This paper proposes a vegetation-water system that incorporates a competition term. Specifically, building upon the system with saturated water uptake, we introduce a parameter capturing the

intraspecific competition effect into the system. This modification more directly illustrates the coupled dynamics between vegetation and water, as well as the mechanistic role of intraspecific vegetation competition:

$$\begin{cases} \dfrac{\partial w}{\partial t} = a - w - \dfrac{pwn^2}{1+\sigma n+n^2} + d_1\Delta w, & x \in \Omega, t > 0, \\ \dfrac{\partial n}{\partial t} = \dfrac{wn^2}{1+\sigma n+n^2} - bn + d_2\Delta n, & x \in \Omega, t > 0, \\ \dfrac{\partial w}{\partial v} = \dfrac{\partial n}{\partial v} = 0, & x \in \partial\Omega, t > 0, \\ (w_0(x,0), n_0(x,0)) \not\equiv (0,0), & x \in \bar{\Omega}. \end{cases} \tag{1.5}$$

The first equation describes the dynamics of water content, where w denotes water density, a is the water input rate, primarily from precipitation, and the term $\frac{pwn^2}{1+\sigma n+n^2}$ represents the loss of water due to uptake by vegetation. The second equation governs the change mechanism of vegetation biomass, where n represents vegetation biomass, the parameter σ represents the intensity of internal competition among organisms, the absorbed water $\frac{wn^2}{1+\sigma n+n^2}$ is used for self-growth, and represents vegetation death due to other reasons. From a biological background, all parameters in the system are non-negative constants. This paper mainly conducts qualitative analysis on the positive steady-state solutions of system (1.5) and focuses on discussing the system

$$\begin{cases} -d_1\Delta v = a - w - \dfrac{pwn^2}{1+\sigma n+n^2}, & x \in \Omega, \\ -d_2\Delta n = \dfrac{wn^2}{1+\sigma n+n^2} - bn, & x \in \Omega, \\ \dfrac{\partial w}{\partial v} = \dfrac{\partial n}{\partial v} = 0, & x \in \partial\Omega. \end{cases} \tag{1.6}$$

The innovation of this study lies in incorporating both water absorption saturation and intraspecific competition into the vegetation-water system, overcoming the limitation that existing models usually neglect density-dependent competition. In arid and semi-arid regions, the nonlinear saturation characteristics and resource competition among individuals jointly determine the overall stability of the ecosystem. This study more comprehensively reveals the synergistic effects between vegetation water uptake capacity and intraspecific competition, and more accurately characterizes the complex hydrological feedback mechanisms between vegetation and water in desertification-prone areas, providing theoretical support that is more consistent with actual ecological processes for understanding vegetation pattern formation, steady-state transitions, and degradation-recovery regimes in arid zones. Meanwhile, the system exhibits richer dynamical behaviors, which significantly increases the difficulty in analyzing its steady-state structure, bifurcation characteristics, and Turing instability mechanism. Therefore, this study not only improves the modeling framework of vegetation-water systems from an ecological perspective, but also has important theoretical and practical significance for revealing the instability mechanism of arid ecosystems and guiding desertification prevention and ecological restoration practices. The research framework is as follows: First, using the comparison principle, we thoroughly investigate the global stability of the boundary equilibrium. Subsequently, we further examine the impact of diffusion on the stability and Turing instability of the positive equilibrium. By applying the maximum principle, we establish a priori

estimates for non-negative solutions and conduct a qualitative analysis of non-constant steady-state solutions. Taking d_1 as the bifurcation parameter, we analyze the local steady-state bifurcations in the cases of simple eigenvalues and double eigenvalues, and clarify the basis for determining the direction of local bifurcations.

The structure of the paper is set as follows: In the first part, we analyze the global stability of the boundary equilibrium and investigate the existence conditions and stability of positive equilibria. The second part is devoted to establishing a priori estimates for non-negative solutions. The third part focuses on the steady-state bifurcation analysis, including the study of local bifurcation, global bifurcation, and bifurcation direction. In the fourth part, we present spatiotemporal diagrams of vegetation patterns through numerical simulations and analyze the influence of different parameters on the spatiotemporal dynamics of vegetation.

2. Materials and methods

2.1. Global stability of boundary equilibrium and Turing instability of positive equilibrium

In this section, we discuss the global stability of the boundary equilibrium of system (1.5) using the comparison principle, and explore the related conclusions on the stability and Turing instability of the positive equilibrium under the diffusion system.

2.1.1. Global stability

In this subsection, we first study the stability of the equilibrium under the ordinary differential system, and then analyze the global stability of the boundary equilibrium.

First, we discuss the following non-diffusion system

$$\begin{cases} \dfrac{\mathrm{d}w}{\mathrm{d}t} = a - w - \dfrac{pwn^2}{1+\sigma n+n^2}, & t > 0, \\ \dfrac{\mathrm{d}n}{\mathrm{d}t} = \dfrac{wn^2}{1+\sigma n+n^2} - bn, & t > 0. \end{cases} \tag{2.1}$$

A straightforward calculation shows that system (2.1) possesses three equilibria: the boundary equilibrium $E_0 = (a, 0)$ and two interior equilibria. $E_0 = (a, 0)$ is the unique boundary equilibrium, and it is locally asymptotically stable [18]. Throughout the paper, we always assume the following conditions hold:

$$a > \sigma b, \quad (a-\sigma b)^2 - 4b^2(1+p) > 0,$$

where system (2.1) has two positive equilibrium $E_1 = (w_1, n_1)$ and $E_2 = (w_2, n_2) = (w^*, n^*)$, which gives the following:

$$E_1 = \left(a + \frac{-pb(a-\sigma b) + pb\sqrt{(a-\sigma b)^2 - 4b^2(1+p)}}{2(b+pb)}, \quad \frac{(a-\sigma b) - \sqrt{(a-\sigma b)^2 - 4b^2(1+p)}}{2(b+pb)} \right) \tag{2.2}$$

and the other equilibrium is

$$E_2 = \left(a + \frac{-pb(a-\sigma b) - pb\sqrt{(a-\sigma b)^2 - 4b^2(1+p)}}{2(b+pb)}, \quad \frac{(a-\sigma b) + \sqrt{(a-\sigma b)^2 - 4b^2(1+p)}}{2(b+pb)} \right) \tag{2.3}$$

and from system (2.1), we obtain $w^* = \dfrac{b}{n^*} + b(\sigma + n^*)$.

Lemma 2.1 ([28]). *Let $f \in C^1([0,\infty]), d > 0, \gamma \geq 0$, and $T \geq 0$ be constants, Ω be a bounded domain in R^N with smooth boundary $\partial\Omega$, and ν be the outer normal vector on $\partial\Omega$. Suppose that the function $\omega \in C^{2,1}(\Omega \times (T,\infty)) \cap C^{1,0}\left(\bar{\Omega} \times [T,\infty)\right)$ is positive, then the hold:*
(i) If ω satisfies

$$\begin{cases} \omega_t - d\Delta\omega \leq (\geq)\, \omega^{1+\gamma} f(\omega)(c-\omega), (x,t) \in \Omega \times (T,\infty), \\ \dfrac{\partial \omega}{\partial \nu} = 0, (x,t) \in \partial\Omega \times (T,\infty), \end{cases}$$

with $c > 0$ being a constant, then $\limsup\limits_{t\to\infty} \max\limits_{\bar{\Omega}} (\cdot,t) \leq c$ ($\liminf\limits_{t\to\infty} \min\limits_{\bar{\Omega}} (\cdot,t) \geq c$).

(ii) If ω satisfies

$$\begin{cases} \omega_t - d\Delta\omega \leq \omega^{1+\gamma} f(\omega)(c-\omega), (x,t) \in \Omega \times (T,\infty), \\ \dfrac{\partial \omega}{\partial \nu} = 0, (x,t) \in \partial\Omega \times (T,\infty), \end{cases}$$

with $c \leq 0$ being a constant, then $\limsup\limits_{t\to\infty} \max\limits_{\bar{\Omega}} (\cdot,t) \leq 0$.

Next, we analyze the global stability of the boundary equilibrium $(a,0)$ based on Lemma 2.1.

Theorem 2.2. *If $a < b\sigma$, the unique boundary equilibrium $(a,0)$ of system (1.5) is globally stable.*

Proof. For any initial value $(w_0(x,0), n_0(x,0)) \not\equiv (0,0)$, $x \in \bar{\Omega}$, we know that the corresponding solution $(w(x,t), n(x,t))$ of system (1.5) satisfies $(w(x,t), n(x,t)) \geq (0,0)$ by the maximum principle. From the first equation of system (1.5), it follows that

$$\omega_t - d_1\omega_{xx} \leq a - w$$

Then, by Lemma 2.1, it can be directly proved that $\limsup\limits_{t\to\infty} \max\limits_{x\in\bar{\Omega}} \omega(x,t) \leq a$. Therefore, $\forall \varepsilon > 0$, there exists $T(\varepsilon) \gg 1$ such that when $x \in \bar{\Omega}, t \geq T(\varepsilon)$, $w(x,t) \leq a + \varepsilon$. Then, for $x \in \bar{\Omega}$ and $t \geq T(\varepsilon)$, the second equation of system (1.5) gives

$$n_t - d_2 n_{xx} \leq \frac{(a+\varepsilon)n^2}{1+\sigma n + n^2} - bn = \frac{(a+\varepsilon-b\sigma)(-n^\varepsilon n^3 + n^2 - n^\varepsilon n)}{1+\sigma n + n^2},$$

where

$$n_\varepsilon = \frac{b}{a+\varepsilon-b\sigma}.$$

If $a < b\sigma$, then for sufficiently small ε, $n^\varepsilon < 0$. By Lemma 2.1, we get $\limsup\limits_{t\to\infty} \max\limits_{\bar{\Omega}} n(x,t) \leq 0$. Noting that $n(x,t) \geq 0$, we have $\lim\limits_{t\to\infty} n(x,t) = 0$.

Since $w(x,t) \geq 0$ and $\lim\limits_{t\to\infty} \frac{pwn^2}{1+\sigma n+n^2} = 0$, $\forall \varepsilon_1 \in (0,1)$, there exists $T(\varepsilon_1) > T(\varepsilon)$ such that $\frac{pwn^2}{1+\sigma n+n^2} \leq \varepsilon_1$ when $t \geq T(\varepsilon_1)$. Using the first equation of system (1.5), we obtain

$$w_t - d_1 w_{xx} \geq a - \varepsilon_1 - w.$$

Lemma 2.1 implies $\liminf_{t\to\infty} \min_{x\in\bar{\Omega}} \omega(x,t) \geq a - \varepsilon_1$. Due to the arbitrariness of ε_1, we have $\liminf_{t\to\infty} \min_{x\in\bar{\Omega}} \omega(x,t) \geq a$. Combining with $\limsup_{t\to\infty} \max_{x\in\bar{\Omega}} \omega(x,t) \leq a$, we get $\lim_{t\to\infty} \omega(x,t) = a, \forall x \in \bar{\Omega}$.

In conclusion,

$$\lim_{t\to\infty}(w(x,t), n(x,t)) = (a, 0), \quad x \in \bar{\Omega}.$$

Thus, the boundary equilibrium $E_0 = (a, 0)$ is globally asymptotically stable. This completes the proof. □

2.1.2. Turing instability

This subsection mainly discusses the stability of the positive equilibrium of the reaction-diffusion system (1.5) and presents the results of Turing instability.

The Jacobian matrix of system (2.1) at (w^*, n^*) is as follows:

$$J = \begin{pmatrix} -1 - \dfrac{p(n^*)^2}{1+\sigma n^* + (n^*)^2} & -\dfrac{pb(\sigma n^* + 2)}{1+\sigma n^* + (n^*)^2} \\ \dfrac{(n^*)^2}{1+\sigma n^* + (n^*)^2} & \dfrac{b(1-(n^*)^2)}{1+\sigma n^* + (n^*)^2} \end{pmatrix}, \tag{2.4}$$

where its characteristic equation is

$$\mu^2 - TrJ\mu + DetJ = 0, \tag{2.5}$$

where

$$TrJ = \frac{(-p-b-1)(n^*)^2 - \sigma n^* + (b-1)}{1+\sigma n^* + (n^*)^2},$$

$$DetJ = \frac{b\left[(1+p)(n^*)^2 - 1\right]}{1+\sigma n^* + (n^*)^2}.$$

Since $n_1 n_2 = \dfrac{1}{1+p}$, we have

$$(1+p)n_1^2 - 1 = (1+p)n_1^2 - (1+p)n_1 n_2 = (1+p)n_1(n_1 - n_2) < 0,$$

$$(1+p)n_2^2 - 1 = (1+p)n_2^2 - (1+p)n_1 n_2 = (1+p)n_2(n_2 - n_1) > 0.$$

Thus,

$$DetJ(E_1) < 0, DetJ(E_2) > 0.$$

Since E_1 is always unstable, we focus on the stability of $E_2 = (w_2, n_2) = (w^*, n^*)$.

Let

$$\sigma_0 := \sigma_0(\sigma^*) = (p-1-b)n^* + \frac{b-1}{n^*}.$$

The following lemma can be easily obtained.

Lemma 2.3. *If $\sigma^* > \sigma_0$, the positive equilibrium point (w^*, n^*) is locally asymptotically stable for system (2.1). If $0 < \sigma^* < \sigma_0$, the positive equilibrium point (w^*, n^*) is unstable for system (2.1).*

Proof. If $\sigma^* > \sigma_0$, then Tr$J < 0$. Since Tr$J < 0$ and Det$J > 0$ are satisfied, (w^*, n^*) is locally asymptotically stable; if $0 < \sigma^* < \sigma_0$, then Tr$J > 0$ and Det$J > 0$, so (w^*, n^*) is unstable. This completes the proof. □

Next, we discuss the stability of (w^*, n^*) in system (1.5). Let

$$0 = \lambda_0 < \lambda_1 < \lambda_2 < \cdots < \lambda_i < \ldots$$

be the eigenvalues of $-\Delta$ on Ω satisfying the homogeneous Neumann boundary conditions, where the multiplicity of λ_i is $m_i \geq 1$. Define the set of orthogonal eigenfunctions corresponding to λ_i as $\{\phi_{ij}\}$, and $\phi_i = \phi_{i1}$. Then, $\{\phi_{ij}\}, i \geq 0, 1 \leq j \leq m_i$ forms a complete orthogonal basis in $L^2(\Omega)$.

The linearization of system (1.5) at (w^*, n^*) is

$$\begin{pmatrix} w_t \\ n_t \end{pmatrix} = L\begin{pmatrix} w \\ n \end{pmatrix} := \begin{pmatrix} -1 - \dfrac{pn^{*2}}{1+\sigma n^* + n^{*2}} + d_1\Delta & -\dfrac{pb(\sigma n^* + 2)}{1+\sigma n^* + n^{*2}} \\ \dfrac{n^{*2}}{1+\sigma n^* + n^{*2}} & \dfrac{b(1-n^{*2})}{1+\sigma n^* + n^{*2}} + d_2\Delta \end{pmatrix}\begin{pmatrix} w \\ n \end{pmatrix}, \tag{2.6}$$

supposing μ is an eigenvalue of the linear operator L, with corresponding eigenfunction $(\Phi, \Psi)^T$. Consider the following:

$$\Phi = \sum_{0\leq i\leq\infty, 1\leq j\leq m_i} a_{ij}\phi_{ij} \ \ and \ \ \Psi = \sum_{0\leq i\leq\infty, 1\leq j\leq m_i} b_{ij}\phi_{ij}.$$

Substituting into the eigenvalue problem $L\begin{pmatrix} \Phi \\ \Psi \end{pmatrix} = \mu\begin{pmatrix} \Phi \\ \Psi \end{pmatrix}$, we obtain

$$\begin{pmatrix} -1 - \dfrac{pn^{*2}}{1+\sigma n^* + n^{*2}} + d_1\Delta & -\dfrac{pb(\sigma n^* + 2)}{1+\sigma n^* + n^{*2}} \\ \dfrac{n^{*2}}{1+\sigma n^* + n^{*2}} & \dfrac{b(1-n^{*2})}{1+\sigma n^* + n^{*2}} + d_2\Delta \end{pmatrix}\begin{pmatrix} \Phi \\ \Psi \end{pmatrix} = \mu\begin{pmatrix} \Phi \\ \Psi \end{pmatrix},$$

direct calculation gives

$$\sum_{0\leq i<\infty, 1\leq j\leq m_i} \begin{pmatrix} -1 - \dfrac{pn^{*2}}{1+\sigma n^* + n^{*2}} - d_1\lambda_i - \mu & -\dfrac{pb(\sigma n^* + 2)}{1+\sigma n^* + n^{*2}} \\ \dfrac{n^{*2}}{1+\sigma n^* + n^{*2}} & \dfrac{b(1-n^{*2})}{1+\sigma n^* + n^{*2}} - d_2\lambda_i - \mu \end{pmatrix}\begin{pmatrix} a_{ij} \\ b_{ij} \end{pmatrix}\phi_{ij} = 0,$$

for non-trivial solutions $(a_{ij}, b_{ij})^T \neq (0, 0)^T$, the determinant of the coefficient matrix must vanish. Thus, μ is an eigenvalue of the linear operator L if and only if, for some $i \geq 0$, it satisfies the characteristic equation

$$\mu^2 - T_i\mu + D_i = 0, \tag{2.7}$$

for $i = 0, 1, 2, \cdots$,where

$$T_i = -(d_1 + d_2)\lambda_i + \frac{(-p-b-1)n^{*2} - \sigma n^* + (b-1)}{1+\sigma n^* + n^{*2}},$$

$$D_i = d_1 d_2 \lambda_i^2 + \left(\frac{1 + \sigma n^* + (p+1)n^{*2}}{1 + \sigma n^* + n^{*2}} d_2 - \frac{b(1 - n^{*2})}{1 + \sigma n^* + n^{*2}} d_1 \right) \lambda_i + \frac{b\left[(1+p)n^{*2} - 1\right]}{1 + \sigma n^* + n^{*2}},$$

obviously, for all $i \geq 0, T_i < 0$, and $D_0 > 0$. Let $z_0 = \frac{1+\sigma n^* + (p+1)n^{*2}}{b(1-n^{*2})}$.

When $\frac{d_1}{d_2} \leq z_0$, $D_i > 0$ and (w^*, n^*) is locally asymptotically stable for system (1.5): When $\frac{d_1}{d_2} > z_0$, consider the following formula:

$$\begin{aligned} \Delta_1 = & \left[\frac{b(1 - n^{*2})}{1 + \sigma n^* + n^{*2}} \right]^2 d_1^2 + \left[\frac{1 + \sigma n^* + (p+1)n^{*2}}{1 + \sigma n^* + n^{*2}} \right]^2 d_2^2 \\ & - \frac{2b(1 - n^{*2})(1 + \sigma n^* + pn^{*2} + n^{*2}) + 4b\left[(1+p)n^{*2} - 1\right]}{1 + \sigma n^* + n^{*2}} d_1 d_2. \end{aligned}$$

Consider the quadratic function defined by

$$\begin{aligned} f(z) = & \left[\frac{b(1 - n^{*2})}{1 + \sigma n^* + n^{*2}} \right]^2 z^2 + \left[\frac{1 + \sigma n^* + (p+1)n^{*2}}{1 + \sigma n^* + n^{*2}} \right]^2 \\ & - \frac{2b(1 - n^{*2})(1 + \sigma n^* + pn^{*2} + n^{*2}) + 4b\left[(1+p)n^{*2} - 1\right]}{1 + \sigma n^* + n^{*2}} z, \end{aligned}$$

where $z = \frac{d_1}{d_2}$. The discriminant of $f(z)$ is given by

$$\Delta_2 = \frac{S^{*2}}{(1 + \sigma n^* + n^{*2})^2} - 4\left[\frac{b(1 - n^{*2})}{1 + \sigma n^* + n^{*2}} \frac{1 + \sigma n^* + (p+1)n^{*2}}{1 + \sigma n^* + n^{*2}} \right]^2,$$

where $S = 2b(1 - n^{*2})(1 + \sigma n^* + pn^{*2} + n^{*2}) + 4b\left[(1+p)n^{*2} - 1\right]$.

After calculation, we find $\Delta_2 > 0$. Therefore, the equation $f(z) = 0$ has two distinct real roots, z_1 and z_2, given by

$$z_1 = \frac{S(1 + \sigma n^* + n^{*2}) - \sqrt{\left[S(1 + \sigma n^* + n^{*2})\right]^2 - 4b^2(1 - n^{*2})^2(1 + \sigma n^* + pn^{*2} + n^{*2})}}{2b^2(1 - n^{*2})^2},$$

$$z_2 = \frac{S(1 + \sigma n^* + n^{*2}) + \sqrt{\left[S(1 + \sigma n^* + n^{*2})\right]^2 - 4b^2(1 - n^{*2})^2(1 + \sigma n^* + pn^{*2} + n^{*2})}}{2b^2(1 - n^{*2})^2}.$$

Furthermore, calculation shows that $z_0 < z_1 < z_2$. When $z_0 < \frac{d_1}{d_2} < z_1$, we have $f(z) < 0$, and consequently $D_i > 0$ for all $i \geq 0$. When $z_1 < \frac{d_1}{d_2} < z_2$, we also have $f(z) < 0$ and $D_i > 0$ for all $i \geq 0$. This means that when $z_0 < \frac{d_1}{d_2} < z_2$, (w^*, n^*) is locally asymptotically stable for system (1.5).

In summary, when $0 < \frac{d_1}{d_2} < z_2$, the equilibrium point (w^*, n^*) is locally asymptotically stable for system (1.5). We obtain the following result.

Theorem 2.4. *Suppose $\sigma^* > \sigma_0$. The stability of the equilibrium (w^*, n^*) of system (1.5) is locally asymptotically stable when $0 < \frac{d_1}{d_2} < z_2$.*

We now discuss the stability of the equilibrium (w^*, n^*) when $\frac{d_1}{d_2} > z_2$. In this case, $\Delta_1 > 0$, implying that the equation $D_i = 0$ admits two positive solutions:

$$\lambda_-(d_1, d_2) = \frac{t - \sqrt{t^2 - 4d_1d_2A}}{2d_1d_2}, \quad \lambda_+(d_1, d_2) = \frac{t + \sqrt{t^2 - 4d_1d_2A}}{2d_1d_2},$$

where

$$t = sd_1 + cd_2, \quad s = \frac{b(1 - n^{*2})}{1 + \sigma n^* + n^{*2}}, \quad c = -\frac{1 + \sigma n^* + (p + 1)n^{*2}}{1 + \sigma n^* + n^{*2}} < 0, \quad A = \frac{b\left[(1 + p)n^{*2} - 1\right]}{1 + \sigma n^* + n^{*2}}.$$

Letting

$$Y(d_1) = s + \frac{cd_2}{d_1} + \sqrt{\left(s + \frac{cd_2}{d_1}\right)^2 - \frac{4d_2A}{d_1}},$$

the derivative of $Y(d_1)$ is

$$Y'(d_1) = -\frac{cd_2}{d_1^2} + \frac{-cd_2\left(s + \frac{cd_2}{d_1}\right) + 2d_2A}{\sqrt{(sd_1 + cd_2)^2 + 4d_1d_2A}}.$$

Since $d_1/d_2 > z_2 > z_0 = -c/s$, we have $sd_1 + cd_2 > 0$. Because $c < 0$, $Y'(d_1) > 0$ for all d_1. Therefore, $\lambda_-(d_1, d_2)$ is increasing with respect to d_1. Let

$$\Phi_1 = \{\lambda \mid \lambda > 0, \lambda_-(d_1, d_2) < \lambda < \lambda_+(d_1, d_2)\}, \quad \Phi_2 = \{\lambda_1, \lambda_2, \lambda_3, \dots\}.$$

Now, d_2 and let $d_1 \to +\infty$. Then,

$$\lim_{d_1 \to +\infty} \lambda_-(d_1, d_2) = 0, \quad \lim_{d_1 \to +\infty} \lambda_+(d_1, d_2) = \frac{s}{d_2} = \frac{b(1 - n^{*2})}{(1 + \sigma n^* + n^{*2})d_2},$$

Thus when d_1 is sufficiently large,

$$0 < \lambda_+(d_1, d_2) < \frac{b(1 - n^{*2})}{(1 + \sigma n^* + n^{*2})d_2}.$$

If $\lambda_1 \geq \frac{b(1-n^{*2})}{(1+\sigma n^*+n^{*2})d_2}$, then $\Phi_1 \cap \Phi_2 = \varnothing$ and $D_i > 0$ for all $i \in N^+$. Therefore, the equilibrium point (w^*, n^*) is locally asymptotically stable for system (1.5), and we can obtain the following theorem.

Theorem 2.5. *When $\sigma^* > \sigma_0$, there exists a sufficiently large $\tilde{d}_1$ such that $d_1 > \tilde{d}_1$.*
(i) If $\lambda_1 \geq \frac{b(1-n^{*2})}{(1+\sigma n^*+n^{*2})d_2}$, then the equilibrium (w^*, n^*) of system (1.5) is asymptotically stable.
(ii) If $\lambda_1 < \frac{b(1-n^{*2})}{(1+\sigma n^*+n^{*2})d_2}$, then the equilibrium (w^*, n^*) is Turing unstable.

Fix d_1 and let $d_2 \to 0$. Then, we have

$$\lim_{d_2 \to 0} \lambda_-(d_1, d_2) = \frac{A}{sd_1} = \frac{(1 + p)n^{*2} - 1}{(1 - n^{*2})d_1}, \quad \lim_{d_2 \to 0} \lambda_+(d_1, d_2) = +\infty.$$

Therefore, there exists a sufficiently small $\widetilde{d_2} > 0$ such that if $0 < d_2 < \widetilde{d_2}$, $\Phi_1 \cap \Phi_2 \neq \varnothing$. Under these conditions, the equilibrium point (w^*, n^*) is unstable in system (1.5), which may give rise to Turing instability.

Theorem 2.6. *Assume that $\sigma^* > \sigma_0$. For sufficiently small $\widetilde{d_2}$,if $d_2 < \widetilde{d_2}$, the equilibrium (w^*, n^*) of system (1.5) becomes Turing unstable.*

Proof. From Theorem 2.4, we know that when d_1/d_2 is small, (w^*, n^*) is asymptotically stable. Theorem 2.6 proves that (w^*, n^*) is Turing unstable when d_2 is small, and from Theorem 2.6, when d_1 is large, the stability of (w^*, n^*) depends on the vegetation region. For the case where d_1 is large, (w^*, n^*) is asymptotically stable when the vegetation region is small, and Turing instability occurs when the vegetation region is large. In fact, the stability or Turing instability of (w^*, n^*) in system (1.5) does not require d_1 to be sufficiently large.

When $d_2\lambda_1 \geq \dfrac{b(1-n^{*2})}{1+\sigma n^*+n^{*2}}$,

$$D_i = d_1 d_2 \lambda_i \left(d_2\lambda_i - \frac{b(1-n^{*2})}{1+\sigma n^*+n^{*2}} \right) + \frac{1+\sigma n^*+(p+1)n^{*2}}{1+\sigma n^*+n^{*2}} d_2\lambda_i + \frac{b\left[(1+p)n^{*2}-1\right]}{1+\sigma n^*+n^{*2}} > 0, \quad i \geq 0,$$

which means (w^*, n^*) is locally asymptotically stable for system (1.5).

Assume $d_2\lambda_1 \leq \dfrac{b(1-n^{*2})}{1+\sigma n^*+n^{*2}}$, and define i_0 as the largest positive integer such that

$$d_2\lambda_i < \frac{b(1-n^{*2})}{1+\sigma n^*+n^{*2}}, \quad 1 \leq i \leq i_0. \tag{2.8}$$

Define a critical diffusion coefficient $\widehat{d_1} = \widehat{d_1}(s, p, b, d_2, \Omega) = \min_{1\leq i\leq i_0} d_{1,i}$, where

$$(Y): d_{1,i} = \frac{\left[1+\sigma n^*+(p+1)n^{*2}\right] d_2\lambda_i + b\left[(1+p)n^{*2}-1\right]}{b(1-n^{*2})\lambda_i - d_2\lambda_i^2(1+\sigma n^*+n^{*2})}. \tag{2.9}$$

For $1 \leq i \leq i_0$, we have $d_2\lambda_1 < \frac{b(1-n^{*2})}{1+\sigma n^*+n^{*2}}$; and, if $0 < d_1 < \widehat{d_1}$, then for $1 \leq i \leq i_0$, we have $d_1 < d_{1,i}$, which means $D_i > 0$. For $i > i_0$, we have $d_2\lambda_i \geq \frac{b(1-n^{*2})}{1+\sigma n^*+n^{*2}}$, which also implies $D_i > 0$. Therefore, $D_i > 0$ for all $i \geq 1$, and (w^*, n^*) is asymptotically stable for system (1.5).

Conversely, if $d_2\lambda_1 < \frac{b(1-n^{*2})}{1+\sigma n^*+n^{*2}}$ and $d_1 > \widehat{d_1}$, let the minimum value in (2.8) be achieved at $j \in [1, i_0]$ and $d_1 > d_{1,j}$, which means $D_j < 0$. Therefore, the equilibrium point (w^*, n^*) is unstable, and Turing instability occurs in system (1.5). Thus, we obtain the following result. □

Theorem 2.7. *Assume $\sigma^* > \sigma_0$.*
(i) If $0 < d_1 < \widehat{d_1}$ holds and conditions $d_2\lambda_1 \geq \frac{b(1-n^{*2})}{1+\sigma n^*+n^{*2}}$, $d_2\lambda_1 < \frac{b(1-n^{*2})}{1+\sigma n^*+n^{*2}}$ are satisfied, then the equilibrium point (w^*, n^*) is asymptotically stable of system (1.5).
(ii) If $d_1 > \widehat{d_1}$ holds and condition $d_2\lambda_1 < \frac{b(1-n^{*2})}{1+\sigma n^*+n^{*2}}$ is satisfied, then the equilibrium point (w^*, n^*) is unstable, and the system (1.5) is Turing instable.

2.2. A priori estimates

In this section, we derive a priori estimates for the non-negative solutions of system (1.5). Let $\bar{f} = \frac{1}{|\Omega|}\int_\Omega f \mathrm{d}x$. First, we present the following two lemmas.

Lemma 2.8 ([29]). *Let Ω be a bounded Lipschitz domain in $\mathbb{R}^N$, and Λ be a non-negative constant. Assume $v \in W^{1,2}$ is a non-negative weak solution to the following inequality:*

$$-\Delta v + \Lambda v \geq 0, \quad x \in \Omega, \quad \frac{\partial v}{\partial \nu} \leq 0, \quad x \in \partial\Omega.$$

Then, for any $q \in \left[1, \frac{n}{n-2}\right)$, there exists a constant C_0, which depends only on q, Λ, and Ω, such that

$$\|v\|_q(\Omega) \leq C_0 \inf_{\Omega} v.$$

Lemma 2.9 ([29]). *Let $g \in C\left(\bar{\Omega} \times R^1\right)$.*
(i) Suppose that $\omega(x) \in C^2(\Omega) \cap C^1\left(\bar{\Omega}\right)$ and satisfies

$$\Delta\omega + g(x, \omega(x)) \geq 0, \quad x \in \Omega, \quad \frac{\partial \omega}{\partial \nu} \leq 0, \quad x \in \partial\Omega.$$

If $\omega(x_0) = \max_{\bar{\Omega}} \omega(x)$, then $g(x_0, \omega(x_0)) \geq 0$.
(ii) Suppose that $\omega(x) \in C^2(\Omega) \cap C^1\left(\bar{\Omega}\right)$ and meets

$$\Delta\omega + g(x, \omega(x)) \leq 0, \quad x \in \Omega, \quad \frac{\partial \omega}{\partial \nu} \geq 0, \quad x \in \partial\Omega.$$

If $\omega(x_0) = \min_{\bar{\Omega}} \omega(x)$, then $g(x_0, \omega(x_0)) \leq 0$.

Now, assume $w, n \in C^2(\Omega) \cap C^1(\bar{\Omega})$ and (w, n) is a non-negative solution of system (1.5). By the maximum principle for elliptic equations, $(w, n) > 0$ on $\bar{\Omega}$. Now, we present the a priori estimates for the non-negative solutions of system (1.5).

Theorem 2.10. *For non-negative solution pair (w, n) of system (1.5), it follows that*

$$\frac{a\left[(pbd_2)^2 + \sigma(pbd_2)(sbd_1 + sd_2) + (sbd_1 + sd_2)^2\right]}{(pbd_2)^2 + \sigma(pbd_2)(sbd_1 + sd_2) + (sbd_1 + sd_2)^2(p+1)} \leq w(x) \leq a,$$

$$\frac{(a - \bar{w})|\Omega|}{pbc_0} \leq n(x) \leq \frac{ad_1}{pd_2} + \frac{a}{pb}.$$

The detailed derivation is presented in Appendix A.

2.3. The steady-state bifurcation

In this section, we discuss the existence of non-trivial positive solutions of system (1.5) in one-dimensional space. Assume $\Omega = (0, \pi)$, and the results can be generalized to higher-dimensional spatial regions.

Taking d_1 as the bifurcation parameter, we prove the existence of non-trivial positive solutions bifurcating from (w^*, n^*). Consider the following elliptic system:

$$\begin{cases} -d_1 w'' = a - w - \dfrac{pwn^2}{1 + \sigma n + n^2}, & x \in (0, \pi), \\ -d_2 n'' = \dfrac{wn^2}{1 + \sigma n + n^2} - bn, & x \in (0, \pi), \\ w' = n' = 0, & x = 0, \pi. \end{cases} \tag{2.10}$$

In addition, we will discuss the structure and direction of bifurcation solutions. Let $(\tilde{w}, \tilde{n}) = (w - w^*, n - n^*)$, and denote $\tilde{w}, \tilde{n}$ as w, n, respectively. Then, system (2.10) is transformed into the following system:

$$\begin{cases} -d_1 w'' = a - (w + w^*) - \dfrac{p(w + w^*)(n + n^*)^2}{1 + \sigma(n + n^*) + (n + n^*)^2}, & x \in (0, \pi), \\ -d_2 n'' = \dfrac{(w + w^*)(n + n^*)^2}{1 + \sigma(n + n^*) + (n + n^*)^2} - b(n + n^*), & x \in (0, \pi), \\ w' = n' = 0, & x = 0, \pi. \end{cases} \tag{2.11}$$

2.3.1. Local Stability Bifurcation

This subsection focuses on exploring the bifurcation behavior of system (2.11) at steady state, analyzing simple eigenvalues and double eigenvalues respectively: For simple eigenvalues, we employ the Crandall-Rabinowitz theorem for research. For multiple eigenvalues, we determine whether bifurcation phenomena occur by spatial decomposition combined with the implicit function theorem.

Let

$$X = \{(w, n) \in W^{2,2}(0, \pi) \times W^{2,2}(0, \pi) : w' = n' = 0, x = 0, \pi\}, \quad Y = L^2(0, \pi) \times L^2(0, \pi).$$

Define the mapping $F : \mathbb{R}^+ \times X \to Y$ as

$$F(d_1, Q) = \begin{pmatrix} d_1 w'' + a - (w + w^*) - \dfrac{p(w + w^*)(n + n^*)^2}{1 + \sigma(n + n^*) + (n + n^*)^2} \\ d_2 n'' + \dfrac{(w + w^*)(n + n^*)^2}{1 + \sigma(n + n^*) + (n + n^*)^2} - b(n + n^*) \end{pmatrix}, \quad Q = (w, n)^T.$$

Then, the solution of system (2.11) is the zero point of this mapping. Obviously, $F(d_1, (0, 0)) = 0$. Consider the Fréchet derivative of F at $(0, 0)$:

$$L(d_1) = F_Q(d_1, (0, 0)) = \begin{pmatrix} d_1\Delta - 1 - \dfrac{pn^{*2}}{1 + \sigma n^* + n^{*2}} & -\dfrac{pw^* n^*(\sigma n^* + 2)}{(1 + \sigma n^* + n^{*2})^2} \\ \dfrac{n^{*2}}{1 + \sigma n^* + n^{*2}} & d_2\Delta + \dfrac{w^* n^*(\sigma n^* + 2)}{(1 + \sigma n^* + n^{*2})^2} - b \end{pmatrix}, \quad \Delta = \frac{d^2}{dx^2}.$$

Assume $d_2\lambda_1 < \frac{b^2(2+\sigma n^*)}{w^* n^*}$. Then, there exists a maximum positive integer i_0 such that $d_2\lambda_1 < \frac{b^2(2+\sigma n^*)}{w^* n^*}$ holds for $1 \le i \le i_0$. Recall

$$d_{1,i} = \frac{aw^* n^* d_2\lambda_i + abw^* n^* + (2 + \sigma n^*)b^2[(2 + \sigma n^*)(a - w^*) - a]}{w^*[b^2(2 + \sigma n^*)\lambda_i - w^* n^* d_2\lambda_i^2]}, \quad \lambda_i = i^2, 1 \le i \le i_0.$$

We will discuss the existence of non-trivial solutions of $F(d_1, (w, n)) = 0$ near $(d_{1,i}, (0, 0))$. When $i \ne j$, $d_{1,i}$ may or may not be equal to $d_{1,j}$. We mainly discuss two cases: When $d_{1,i} \ne d_{1,j}$ $(i \ne j)$, it corresponds to the simple eigenvalue problem; when $d_{1,i} = d_{1,j}$ $(i \ne j)$, it corresponds to the double eigenvalue problem.

The local bifurcation at simple eigenvalues follows the Rabinowitz bifurcation theory [30].

Theorem 2.11. *When $i \neq j$ ensures that $d_{1,i} \neq d_{1,j}$ for any integers i, j within the interval $[1, i_0]$, $(d_{1,i}, (0,0))$ serves as a bifurcation point for the equation $F(d_1, Q) = 0$. Additionally, for values of $|r|$ that are sufficiently small, there exists a curve of nonconstant solutions $(d_1(r), (w(r), n(r)))$ that satisfy $F(d_1, Q) = 0$ such that*

$$d_1(0) = d_{1,i},\ (w(0), n(0)) = (0,0),\ w(r) = r\phi_i + O(r), n(r) = re_i\phi_i + O(r),$$

in which $d_1(r), w(r)$, and $n(r)$ are functions that are smoothly differentiable with respect to r, $\phi_i = \sqrt{\frac{2}{\pi}}\cos(ix)$, and

$$e_i = -\frac{n^{*2}(1+\sigma n^* + n^{*2})}{(d_2\lambda_i - b)(1+\sigma n^* + n^{*2}) + w^* n^*(\sigma n^* + 2)}.$$

The detailed derivation is presented in Appendix B.

Next, we study the bifurcation from double eigenvalues through spatial decomposition and the implicit function theorem.

Theorem 2.12. *Assume there is a positive integer $i \neq j$ fulfilling $d_{1,i} = d_{1,j} = \tilde{d}_1$. Consider*

$$e_i = -\frac{n^{*2}(1+\sigma n^* + n^{*2})}{(d_2\lambda_i - b)(1+\sigma n^* + n^{*2}) + w^* n^*(\sigma n^* + 2)}, \tag{2.12}$$

$$e_i^* = \frac{pw^* n^*(\sigma n^* + 2)}{(d_2\lambda_i - b)(1+\sigma n^* + n^{*2}) + w^* n^*(\sigma n^* + 2)}, \quad \Phi_i = \begin{pmatrix} 1 \\ e_i \end{pmatrix}\phi_i, \tag{2.13}$$

$$O_1 = -\frac{pn^*(2+\sigma n^*)}{(1+\sigma n^* + n^{*2})^2}e_i - \frac{pb\left[(1+\sigma n^*)(1+\sigma n^* + n^{*2}) - w^* n^*(2+\sigma n^*)(\sigma + 2n^*)\right]^2}{n^{*2}(1+\sigma n^* + n^{*2})^2}e_i^2,$$

$$O_3 = -\frac{pn^*(2+\sigma n^*)}{(1+\sigma n^* + n^{*2})^2}e_j - \frac{pb\left[(1+\sigma n^*)(1+\sigma n^* + n^{*2}) - w^* n^*(2+\sigma n^*)(\sigma + 2n^*)\right]^2}{n^{*2}(1+\sigma n^* + n^{*2})^2}e_j^2,$$

$$O_2 = -\frac{pn^*(2+\sigma n^*)}{(1+\sigma n^* + n^{*2})^2}(e_i + e_j) - \frac{2pb\left[(1+\sigma n^*)(1+\sigma n^* + n^{*2}) - w^* n^*(2+\sigma n^*)(\sigma + 2n^*)\right]}{n^{*2}(1+\sigma n^* + n^{*2})^2}e_i e_j, \tag{2.14}$$

$$X_2 := \{(y,z)^T \in X : \int_0^\pi (y + e_i z)\phi_i dx = \int_0^\pi (y + e_j z)\phi_j dx = 0\}. \tag{2.15}$$

If $1 + e_i e_i^* \neq 0$ and $1 + e_j e_j^* \neq 0$ for $j = 2i$ $(i = 2j)$, then $\left(d_1^*, (0,0)\right)$ is a bifurcation point of $F(d_1, Q) = 0$. Additionally, for $|\xi - \xi_0|$ sufficiently small, we can find a family of non-trivial solutions $\left(d_1(\xi), r(\xi)\left(\cos\xi\Phi_i + \sin\xi\Phi_j + W(\xi)\right)\right)$ of $F(d_1, Q) = 0$ such that $d_1(\xi_0) = d_1^*, r(\xi_0) = 0$, and $W(\xi_0) = 0$, where $d_1(\xi_0), r(\xi_0)$, and $W(\xi_0)$ are smooth functions in relation to ξ, while ξ_0 represents any given constant that meets the specified conditions

$$\tan^2\xi_0 \neq \frac{O_1\left(e_j^* - 1\right)i^2}{O_2\left(e_i^* - 1\right)j^2}, \tag{2.16}$$

$$\left(\tan^2\xi_0 \neq \frac{O_2\left(e_j^* - 1\right)i^2}{O_3\left(e_i^* - 1\right)j^2}\right). \tag{2.17}$$

Proof. From the proof presented in Appendix C,

$$\dim\ker L(\hat{d}_1) = \operatorname{codim} M(L(\hat{d}_1)) = 2.$$

Thus, the Crandall-Rabinowitz bifurcation theory is no longer applicable. Therefore, we consider this problem using the techniques of spatial decomposition and the implicit function theorem.

First we perform the following decomposition. Let $X_1 = \ker L(\hat{d}_1)$, and define the operator P on Y as

$$P\begin{pmatrix} w \\ n \end{pmatrix} = \frac{1}{1+e_i e_i^*}\left[\int_0^\pi (w + e_i^* n)\phi_i dx\right]\Phi_i + \frac{1}{1+e_j e_j^*}\left[\int_0^\pi (w + e_j^* n)\phi_j dx\right]\Phi_j,$$

where $M(P) = \operatorname{span}\{\Phi_i, \Phi_j\} = X_1 \subset Y$, and $P^2 = P$, which indicates that P is a projection from Y to X_1.

Decompose Y as $Y = Y_1 \oplus Y_2$, where $Y_1 = M(P) = X_1$, and $Y_2 = \ker(P) = M(L(\hat{d}_1))$.

Through calculation, we obtain $R(P) = \operatorname{span}\left\{\Phi_{\mathrm{i}}, \Phi_{\mathrm{j}}\right\} = \mathrm{X}_1 \subset \mathrm{Y}, \mathrm{P}^2 = \mathrm{P}$. Therefore, P is the projection from Y to $X_1 \subset Y$. Decompose Y into $Y = Y_1 \oplus Y_2$, where $Y_1 = R(P) = X_1, and\ Y_2 = \ker(P) = R\left(L\left(\tilde{d}_1\right)\right)$. Meanwhile, decompose X as $X = X_1 \oplus X_2$. Moreover, set $X_1 = \operatorname{span}\left\{\Phi_{\mathrm{i}}, \Phi_{\mathrm{j}}\right\}$, and define X_2 according to (2.15).

Then, seek solutions of $F(d_1, Q) = 0$ in the form.

$$Q = r\left(\cos\xi\Phi_i + \sin\xi\Phi_j + W\right), \quad W = (w_1, w_2)^T \in X_2, \tag{2.18}$$

where, $r, \xi \in R$ are parameters.

Next, let $\xi_0 \in R$ and define a nonlinear mapping

$$H(d_1, r, W; \xi) : \mathbb{R}^+ \times \mathbb{R} \times X_2 \times (\xi_0 - \delta, \xi_0 + \delta) \to Y$$

is defined

$$H(d_1, r, W; \xi) = L(d_1)(\cos\xi\Phi_i + \sin\xi\Phi_j + W) + r\begin{pmatrix} \widetilde{F}^1 \\ \widetilde{F}^2 \end{pmatrix},$$

where

$$\begin{aligned}\widetilde{F}^2 = {} & \frac{n^*(2+\sigma n^*)}{(1+\sigma n^* + n^{*2})^2}(\cos\xi\phi_i + \sin\xi\phi_j + w_1)(e_i\cos\xi\phi_i + e_j\sin\xi\phi_j + w_2) \\ & + \frac{1+\sigma n^* - 2n^{*2} - 4\sigma n^{*3} - \sigma^2 n^{*4}}{n^*(1+\sigma n^* + n^{*2})^3}(e_i\cos\xi\phi_i + e_j\sin\xi\phi_j + w_2)^2 + O(|r|),\end{aligned}$$

and $\widetilde{F}^1 = -p\widetilde{F}^2$. Obviously, $H(\hat{d}_1, 0, 0; \xi_0) = 0$. Calculation shows that

$$\begin{aligned}H_{(d_1,r,W)}(\hat{d}_1, 0, 0; \xi_0)(d_1, r, W) = {} & L(\hat{d}_1)W - d_1\lambda_i\cos\xi_0\begin{pmatrix}\phi_i \\ 0\end{pmatrix} - d_1\lambda_j\sin\xi_0\begin{pmatrix}\phi_j \\ 0\end{pmatrix} \\ & + rO_1\cos^2\xi_0\begin{pmatrix}\phi_i^2 \\ -\frac{1}{p}\phi_i^2\end{pmatrix} + rO_2\cos\xi_0\sin\xi_0\begin{pmatrix}\phi_i\phi_j \\ -\frac{1}{p}\phi_i\phi_j\end{pmatrix} \\ & + rO_3\sin^2\xi_0\begin{pmatrix}\phi_j^2 \\ -\frac{1}{p}\phi_j^2\end{pmatrix},\end{aligned}$$

where $O_1, O_2, and\ O_3$ are constants determined by the nonlinear terms in (2.14). □

In the following, we establish that the mapping $H_{(d_1,r,W)}(\hat{d}_1, 0, 0; \xi) : \mathbb{R}^+ \times \mathbb{R} \times X_2 \to Y$, is indeed an isomorphic function. For this purpose, we proceed with a necessary decomposition:

$$\begin{pmatrix} \phi_i \\ 0 \end{pmatrix} = g_i \Phi_i + \begin{pmatrix} w_1 \\ n_1 \end{pmatrix}, \quad \begin{pmatrix} \phi_j \\ 0 \end{pmatrix} = g_j \Phi_j + \begin{pmatrix} w_2 \\ n_2 \end{pmatrix},$$

where

$$\begin{pmatrix} w_1 \\ n_1 \end{pmatrix} = \begin{pmatrix} 1 - g_1 \\ -g_1 e_i \end{pmatrix} \phi_i \in Y_2, \quad g_i = \frac{1}{1 + e_i e_i^*} \neq 0,$$

$$\begin{pmatrix} w_2 \\ n_2 \end{pmatrix} = \begin{pmatrix} 1 - g_2 \\ -g_2 e_j \end{pmatrix} \phi_j \in Y_2, \quad g_j = \frac{1}{1 + e_j e_j^*} \neq 0.$$

The discussion is divided into two cases: $j = 2i$ and $i = 2j$.

Case 1. When $j = 2i$

In this situation, the following integrals hold

$$\int_0^\pi \phi_i^2 dx = \frac{1}{\sqrt{2\pi}}, \quad \int_0^\pi \phi_i \phi_j dx = 0, \quad \int_0^\pi \phi_i^2 dx = \int_0^\pi \phi_j^2 dx = 0,$$

which implies $\begin{pmatrix} -\phi_i^2 \\ \phi_j^2 \end{pmatrix} \in Y_2$. Next, perform the following decomposition:

$$\begin{pmatrix} -\phi_i^2 \\ \phi_j^2 \end{pmatrix} = g_3 \Phi_j + \begin{pmatrix} w_3 \\ n_3 \end{pmatrix}, \quad \begin{pmatrix} -\phi_i \phi_j \\ \phi_i \phi_j \end{pmatrix} = g_4 \Phi_i + \begin{pmatrix} w_4 \\ n_4 \end{pmatrix},$$

$$g_3 = \frac{e_j^* - 1}{e_j e_j^* + 1} \int_0^\pi \phi_i^2 \phi_j dx = \sqrt{\frac{1}{2\pi}} \frac{p - e_j^*}{\pi e_j e_j^* + p} < 0, \quad \begin{pmatrix} w_3 \\ n_3 \end{pmatrix} = \begin{pmatrix} \phi_i^2 - g_3 \phi_j \\ -\frac{1}{p}\phi_i^2 - g_3 e_j \phi_j \end{pmatrix} \in Y_2,$$

$$g_4 = \frac{e_i^* - 1}{e_i e_i^* + 1} \int_0^\pi \phi_i^2 \phi_j dx = \sqrt{\frac{1}{2\pi}} \frac{p - e_i^*}{\pi e_i e_i^* + p} < 0, \quad \begin{pmatrix} w_4 \\ n_4 \end{pmatrix} = \begin{pmatrix} \phi_i \phi_j - g_4 \phi_i \\ -\frac{1}{p}\phi_i \phi_j - g_4 e_i \phi_i \end{pmatrix} \in Y_2.$$

At this point, after rearrangement, we have

$$H_{(d_1,r,W)}(\hat{d}_1, 0, 0; \xi_0)(d_1, r, W) = \mathcal{Y}_1 + \mathcal{Y}_2,$$

where

$$\mathcal{Y}_1 = (-d_1 g_1 \lambda_i \cos\xi_0 + r g_3 O_2 \cos\xi_0 \sin\xi_0)\Phi_i + (-d_1 g_2 \lambda_j \sin\xi_0 + r g_3 O_1 \cos^2\xi_0)\Phi_j \in Y_1,$$

$$\begin{aligned} \mathcal{Y}_2 = {} & L(\hat{d}_1)W - d_1 \lambda_i \cos\xi_0 \begin{pmatrix} w_1 \\ n_1 \end{pmatrix} - d_1 \lambda_j \sin\xi_0 \begin{pmatrix} w_2 \\ n_2 \end{pmatrix} \\ & + r A_1 \cos^2\xi_0 \begin{pmatrix} w_3 \\ n_3 \end{pmatrix} + r A_2 \cos\xi_0 \sin\xi_0 \begin{pmatrix} w_4 \\ n_4 \end{pmatrix} + r A_3 \sin^2\xi_0 \begin{pmatrix} -\phi_j^2 \\ \phi_0^2 \end{pmatrix} \in Y_2. \end{aligned} \tag{2.19}$$

Let

$$H_{(d_1,r,W)}(\hat{d}_1, 0, 0; \xi_0)(d_1, r, W) = 0. \tag{2.20}$$

Since $L(\hat{d}_1)$ is an isomorphism from X_2 to Y_2, (2.20) is equivalent to

$$\begin{cases} (-d_1 g_1 \lambda_i \cos\xi_0 + r g_4 O_2 \cos\xi_0 \sin\xi_0)\Phi_i + (-d_1 g_2 \lambda_j \sin\xi_0 + r g_3 O_1 \cos^2\xi_0)\Phi_j = 0, \\ L(\hat{d}_1)W - d_1\lambda_i \cos\xi_0 \begin{pmatrix} w_1 \\ n_1 \end{pmatrix} - d_1 \lambda_j \sin\xi_0 \begin{pmatrix} w_2 \\ n_2 \end{pmatrix} + r O_1 \cos^2\xi_0 \begin{pmatrix} w_3 \\ n_3 \end{pmatrix} \\ \quad + r O_2 \cos\xi_0 \sin\xi_0 \begin{pmatrix} w_4 \\ n_4 \end{pmatrix} + r O_3 \sin^2\xi_0 \begin{pmatrix} -\phi_i^2 \\ \phi_j^2 \end{pmatrix} = 0. \end{cases} \tag{2.21}$$

From (2.16), the first equation of (2.21) gives: $d_1 = 0, r = 0$. Substituting these into $\mathcal{Y}_2 = 0$, we get $W = 0$, which means $H_{(d_1,r,W)}(\hat{d}_1, 0, 0; \xi_0)$ is injective.

Next, for any $\begin{pmatrix} w \\ n \end{pmatrix} \in Y$, we need to find $(d_1, r, W) \in X$ such that

$$H_{(d_1,r,W)}(\hat{d}_1, 0, 0; \xi_0)(d_1, r, W) = \begin{pmatrix} w \\ n \end{pmatrix}. \tag{2.22}$$

Through the decomposition of Y, there exist $\alpha, \beta \in \mathbb{R}$ and $\begin{pmatrix} w_0 \\ n_0 \end{pmatrix} \in Y_2$ such that

$$\begin{pmatrix} w \\ n \end{pmatrix} = \begin{pmatrix} w_0 \\ n_0 \end{pmatrix} + \alpha\Phi_i + \beta\Phi_j.$$

Substituting the above expression into (2.22).

$$\begin{cases} -d_1 g_1 \lambda_i \cos\xi_0 + r g_4 O_2 \cos\xi_0 \sin\xi_0 = \alpha, \\ -d_1 g_2 \lambda_j \sin\xi_0 + r g_3 O_1 \cos^2\xi_0 = \beta, \\ L(\hat{d}_1)W - d_1\lambda_i \cos\xi_0 \begin{pmatrix} w_1 \\ n_1 \end{pmatrix} - d_1 \lambda_j \sin\xi_0 \begin{pmatrix} w_2 \\ n_2 \end{pmatrix} + r O_1 \cos^2\xi_0 \begin{pmatrix} w_3 \\ n_3 \end{pmatrix} \\ \quad + r O_2 \cos\xi_0 \sin\xi_0 \begin{pmatrix} w_4 \\ n_4 \end{pmatrix} + r O_3 \sin^2\xi_0 \begin{pmatrix} -\phi_i^2 \\ \phi_j^2 \end{pmatrix} = \begin{pmatrix} w_0 \\ n_0 \end{pmatrix}. \end{cases} \tag{2.23}$$

Since (2.16) holds, we have $d_1 = \overline{d}_1$ and $r = \overline{r}$, where

$$d_1 = \overline{d}_1 := \frac{\alpha g_3 O_1 \cos^2\xi_0 - \beta g_4 O_2 \sin\xi_0}{g_2 g_4 \lambda_j O_2 \sin^2\xi_0 - g_1 g_3 \lambda_i O_1 \cos^2\xi_0},$$

$$r = \overline{r} := \frac{\alpha g_2 \lambda_j \sin\xi_0 - \beta g_1 \lambda_i}{g_2 g_4 \lambda_j O_2 \sin^2\xi_0 - g_1 g_3 \lambda_i O_1 \cos^2\xi_0}.$$

Substitute $\overline{d}_1, \overline{r}$ into the third equation of (2.23),

$$\begin{aligned} L(\overline{d}_1)W = &\begin{pmatrix} w_0 \\ n_0 \end{pmatrix} + \overline{d}_1 \lambda_i \cos\xi_0 \begin{pmatrix} w_1 \\ n_1 \end{pmatrix} + \overline{d}_1 \lambda_j \sin\xi_0 \begin{pmatrix} w_2 \\ n_2 \end{pmatrix} \\ &- \overline{r} O_1 \cos^2\xi_0 \begin{pmatrix} w_3 \\ n_3 \end{pmatrix} - \overline{r} O_2 \cos\xi_0 \sin\xi_0 \begin{pmatrix} w_4 \\ n_4 \end{pmatrix} - \overline{r} O_3 \sin^2\xi_0 \begin{pmatrix} -\phi_i^2 \\ \phi_j^2 \end{pmatrix} := \begin{pmatrix} \overline{w} \\ \overline{n} \end{pmatrix} \in Y_2. \end{aligned}$$

This implies

$$W = L^{-1}\begin{pmatrix}\overline{w}\\ \overline{n}\end{pmatrix} \in Y_2.$$

Then,

$$(d_1, r, W) = \left(\overline{d}_1, \overline{r}, L^{-1}\begin{pmatrix}\overline{w}\\ \overline{n}\end{pmatrix}\right)$$

satisfies (2.22), which shows that $H_{(d_1,r,W)}(\overline{d}_1, 0, 0; \xi_0)$ is surjective.

Therefore, $H_{(d_1,r,W)}(\overline{d}_1, 0, 0; \xi_0)$ is an isomorphism from $\mathbb{R}^+ \times \mathbb{R} \times X_2$ to Y. For

$$H(d_1, r, W; \xi) = 0, \tag{2.24}$$

applying the implicit function theorem, we obtain that for sufficiently small $|\xi - \xi_0|$, there exists a family of non-trivial solutions $(d_1(\xi), r(\xi), W(\xi))$ of (4.18) (i.e., $F = 0$) satisfying $d_1(\xi_0) = \overline{d}_1$, $r(\xi_0) = 0$, $W(\xi_0) = 0$, where $d_1(\xi), r(\xi), and\ W(\xi)$ are continuously differentiable functions with respect to ξ, and $W \in X_2$.

Case 2. When $i = 2j$

First,

$$\int_0^\pi \phi_i^2\phi_j dx = 0, \quad \int_0^\pi \phi_i\phi_j^2 dx = \sqrt{\frac{1}{2\pi}} \neq 0.$$

Then, $\begin{pmatrix}-\phi_j^2\\ \phi_i^2\end{pmatrix} \in Y_2$, and we decompose

$$\begin{pmatrix}-\phi_j^2\\ \phi_i^2\end{pmatrix} = g_5\Phi_i + \begin{pmatrix}w_5\\ n_5\end{pmatrix}, \quad \begin{pmatrix}-\phi_i\phi_j\\ \phi_i\phi_j\end{pmatrix} = g_6\Phi_j + \begin{pmatrix}w_6\\ n_6\end{pmatrix},$$

where

$$\begin{pmatrix}w_5\\ n_5\end{pmatrix} = \begin{pmatrix}-\phi_j^2 - g_5\phi_i\\ -\frac{1}{p}\phi_j^2 - g_5 e_i\phi_i\end{pmatrix}, \quad g_5 = \sqrt{\frac{1}{2\pi}}\frac{p - e_i^*}{pe_ie_i^* + p} = g_4,$$

$$\begin{pmatrix}w_6\\ n_6\end{pmatrix} = \begin{pmatrix}-\phi_i\phi_j - c_6\phi_j\\ -\frac{1}{p}\phi_i\phi_j - c_6 e_j\phi_j\end{pmatrix}, \quad c_6 = \sqrt{\frac{1}{2\pi}}\frac{p - e_j^*}{pe_je_j^* + p} = c_3.$$

After rearrangement, we get

$$\begin{aligned}H_{(d_1,r,W)}(\overline{d}_1, 0, 0; \xi_0)(d_1, r, W) = {} & L(\overline{d}_1)W + (-d_1g_1\lambda_i\cos\xi_0 + rg_5O_3\sin^2\xi_0)\Phi_i\\ & + (-d_1g_2\lambda_j\sin\xi_0 + rg_6O_2\cos\xi_0\sin\xi_0)\Phi_j - d_1\lambda_i\cos\xi_0\begin{pmatrix}w_1\\ n_1\end{pmatrix}\\ & - d_1\lambda_j\sin\xi_0\begin{pmatrix}w_2\\ n_2\end{pmatrix} + \overline{r}O_3\sin^2\xi_0\begin{pmatrix}w_5\\ n_5\end{pmatrix} + \overline{r}O_2\cos\xi_0\sin\xi_0\begin{pmatrix}w_6\\ n_6\end{pmatrix}\\ & + \overline{r}O_1\cos^2\xi_0\begin{pmatrix}\phi_j^2\\ -\frac{1}{p}\phi_i^2\end{pmatrix},\end{aligned}$$

where

$$\begin{pmatrix}w_1\\ n_1\end{pmatrix}, \begin{pmatrix}w_2\\ n_2\end{pmatrix}, \begin{pmatrix}w_5\\ n_5\end{pmatrix}, \begin{pmatrix}w_6\\ n_6\end{pmatrix}, \begin{pmatrix}-\phi_i^2\\ \phi_j^2\end{pmatrix} \in Y_2.$$

Since $i = 2j$, similar to the argument in Case 1, if ξ_0 satisfies (2.17), we can prove that the mapping $H_{(d_1,r,W)}(\hat{d}_1, 0, 0; \xi_0)$ is an isomorphism from $\mathbb{R}^+ \times \mathbb{R} \times X_2$ to Y. The proof for this case is completed by applying the implicit function theorem.

When $j \neq 2i$ and $i \neq 2j$, we cannot prove the existence of non-trivial positive solutions of (2.10). In this case, $\int_0^\pi \phi_i^2 \phi_j dx = \int_0^\pi \phi_j^2 \phi_i dx = 0$, which makes

$$\begin{pmatrix} -\phi_i^2 \\ \phi_j^2 \end{pmatrix}, \begin{pmatrix} -\phi_j^2 \\ \phi_i^2 \end{pmatrix}, \text{ and } \begin{pmatrix} -\phi_i\phi_j \\ \phi_i\phi_j \end{pmatrix} \in Y_2,$$

and note that at this time $H_{(d_1,r,W)}(\hat{d}_1, 0, 0; \omega_0) : \mathbb{R}^+ \times \mathbb{R} \times X_2 \to Y$ is not an isomorphism. Therefore, the implicit function theorem cannot be used to obtain existence results for the case $j \neq 2i$ and $i \neq 2j$.

2.3.2. Global structure and orientation of steady-state bifurcations

Next, we further study the global structure of steady-state bifurcation from simple eigenvalues by applying global bifurcation theory.

Lemma 2.13 ([31]). *Suppose X and Y are real Banach spaces, W is an open set in $\mathbb{R} \times X$, $(\mu_0, 0) \in W$, and let $\mathcal{F}$ be a continuously differentiable mapping from W to Y. Assume that*
(i) For all $(\mu, 0) \in W$, $\mathcal{F}(\mu, 0) = 0$;
(ii) $D_w\mathcal{F}(\mu, w)$, the Fréchet derivative, exists and is continuous when (μ, w) is close to $(\mu_0, 0)$;
(iii) For some $(\mu_0, 0) \in W$, $R(D_w\mathcal{F}(\mu_0, 0))$ is closed, $\dim \mathrm{Ker}(D_w\mathcal{F}(\mu_0, 0)) = 1$ *and* $\mathrm{codim} R(D_w\mathcal{F}(\mu_0, 0)) = 1$;
(iv) $D^2_{\mu w}\mathcal{F}(\mu_0, 0)w_0 \notin R(D_w\mathcal{F}(\mu_0, 0))$, where $\mathrm{Ker}(D_w\mathcal{F}(\mu_0, 0))$ *is spanned by w_0. If these conditions are satisfied, let $Z \subset Y$ be any complement of the 1-dimensional space spanned by w_0^*. Then, there exists an open interval $S_1 = (-\varepsilon, \varepsilon)$ and two continuously differentiable functions: $\mu : S_1 \to \mathbb{R}$ satisfying $\mu(0) = \mu_0$, and $\phi : S_1 \to Z$ satisfying $\phi(0) = \phi_0$, to ensure $\mathcal{F}(\mu(s), sw_0 + s\phi(s)) = 0$ holds for $s \in S_1$. Moreover, in a sufficiently small neighborhood of $(\mu, 0)$ in W, the entire solution set of $\mathcal{F}(\mu, w) = 0$ consists of the curve $(\mu(s), sw_0 + s\phi(s))$ and the line $(\mu, 0)$.*
(v) Let C denote the connected complement of S_2, where $S_2 = \{(\mu, w) \in W : \mathcal{F}(\mu, w) = 0, w \neq 0\}$. Meanwhile, when $D_w\mathcal{F}(\mu, w)$ is a Fredholm operator for all $(\mu, w) \in W$, then the curve $(\mu(s), sw_0 + s\phi(s))$ is contained in C, and either C contains a point $(\mu^*, 0)$ satisfying $\mu^* \neq \mu_0$, or C is not compact in W.

All the above conclusions have been proved in Theorem 2.11 of this paper. Then, the conclusion of local bifurcation analysis is generalized to global results. As discussed in [31], Shi and Wang [31] proved that the linear operator is a Fredholm operator. With this established, we can leverage the abstract global bifurcation theorem in [32] to carry out bifurcation analysis directly on these elliptic systems. To depict its global structure more clearly, let G denote the closure of the set of non-trivial solutions of system (2.10), and Y_i denote the connected component of $G \cup (d_{1,j}, (w^*, n^*))$.

Theorem 2.14. *Based on the assumption of Theorem 2.11, the projection of the bifurcation curve Y_i onto the d_1-axis contains $(d_{1,j}, +\infty)$. Moreover, for any integer $j > 0$, if $d_1 > \hat{d}_1$ and $d_1 \neq d_{1,j}$, system (2.10) has at least one non-trivial positive solution.*

Remark 2.15. *Theorem 2.14 only excludes the possibility that Y_i eventually meets some bifurcation points without reaching infinity. Y_i may encounter some bifurcation points and then reach infinity.*

Next, we consider the direction of the steady-state bifurcation from simple eigenvalues in Theorem 2.11.

Define the mapping $F : \mathbb{R}^+ \times X \to Y$ as

$$F(d_1, Q) = \begin{pmatrix} gd_1 w + \tilde{q}(w, n) \\ d_2 n + \tilde{b}(w, n) \end{pmatrix},$$

where

$$\tilde{q}(w,n) = a - (w + w^*) - \frac{p(w + w^*)(n + n^*)^2}{1 + \sigma(n + n^*) + (n + n^*)^2}, \quad \tilde{b}(w,n) = \frac{(w + w^*)(n + n^*)^2}{1 + \sigma(n + n^*) + (n + n^*)^2} - b(n + n^*).$$

By direct calculation, we have

$$\begin{aligned}
\tilde{q}_w(0,0) &= -\frac{pn^{*2}}{1 + \sigma n^* + n^{*2}} - 1, & \tilde{b}_w(0,0) &= \frac{n^{*2}}{1 + \sigma n^* + n^{*2}}, \\
\tilde{q}_n(0,0) &= -\frac{pb(\sigma n^* + 2)}{1 + \sigma n^* + n^{*2}}, & \tilde{b}_n(0,0) &= \frac{b(\sigma n^* + 2) - b}{1 + \sigma n^* + n^{*2}} - b, \\
\tilde{q}_{ww}(0,0) &= -p\tilde{b}_{ww}(0,0) = 0, & \tilde{b}_{ww}(0,0) &= 0, \\
\tilde{q}_{www}(0,0) &= -p\tilde{b}_{www}(0,0) = 0, & \tilde{b}_{www}(0,0) &= 0, \\
\tilde{q}_{wn}(0,0) &= -\frac{pn^*(\sigma n^* + 2)}{(1 + \sigma n^* + n^{*2})^2}, & \tilde{b}_{wn}(0,0) &= \frac{n^*(\sigma n^* + 2)}{(1 + \sigma n^* + n^{*2})^2}, \\
\tilde{q}_{nn}(0,0) &= \frac{p(b\sigma + b\sigma n^* + 4bn^*)}{(1 + \sigma n^* + n^{*2})^2}, & \tilde{b}_{nn}(0,0) &= -\frac{b\sigma + b\sigma n^* + 4bn^*}{(1 + \sigma n^* + n^{*2})^2},
\end{aligned}$$

$$\tilde{q}_{wnn}(0,0) = -p\tilde{b}_{wnn}(0,0) = -\frac{2p + 2p\sigma n + (2\sigma^2 - 2)(1 - n^*)^2 pn^{*2} - (3 + \sigma^2)2pn^{*4} - 2p\sigma n^{*5}}{(1 + \sigma n^* + n^{*2})^4},$$

$$\tilde{q}_{nnn}(0,0) = -p\tilde{b}_{nnn}(0,0) = \frac{2pb\left[2 + \sigma^2 - (\sigma + \sigma^3)n^* - (5 + 3\sigma^2)n^{*2} - 10\sigma n^{*3} - (\sigma^2 + 6)n^{*4} - \sigma n^{*5}\right]}{(1 + \sigma n^* + n^{*2})^4}.$$

Based on Theorem 2.11, we have

$$\dim \ker F_Q\left(d_{1,i}, (0,0)\right) = co\dim M\left(F_Q\left(d_{1,i}, (0,0)\right)\right) = 1,$$

and $\ker F_Q(d_{1,i}, (0,0)) = \text{span}\{\Phi_i\}$. Thus, X and Y can be decomposed as

$$X = \ker F_Q(d_{1,i}, (0,0)) \oplus Z \quad \text{and} \quad Y = M(F_Q(d_{1,i}, (0,0))) \oplus Z',$$

where Z and Z' are the complement spaces of $\ker F_Q(d_{1,i}, (0,0))$ in X and $R(F_Q(d_{1,i}, (0,0)))$ in Y, respectively. From (B.1), we know

$$\langle F_{d_1 Q}(d_{1,i}, (0,0))\Phi_i, \Phi_i^* \rangle = -\lambda_i = -i^2 \neq 0.$$

According to the expression of (2.13) in [29], we can obtain

$$d_1'(0) = -\frac{\langle F_{QQ}(d_{1,i}, (0,0))\Phi_i^2, \Phi_i^* \rangle}{2\langle F_{dQ}(d_{1,i}, (0,0))\Phi_i, \Phi_i^* \rangle}.$$

By calculation, we get

$$\langle F_{QQ}(d_{1,i},(0,0))\Phi_i^2,\Phi_i^*\rangle = (k_i + r_i e_i^*)\int_0^\pi \phi_i^3\,\mathrm{d}x,$$

where $k_i = -pr_i$ and

$$\begin{aligned} r_i &= \tilde{b}_{ww}(\theta,\Omega) + 2\tilde{b}_{wn}(\theta,\Omega)e_i + \tilde{b}_{nn}(\theta,\Omega)e_i^2 \\ &= \frac{1}{(1+\sigma n^* + n^{*2})^2}\left[2n^*(2+\sigma n^*) - (b\sigma + b\sigma n^{*2} + 4bn^*)e_i^2\right]e_i. \end{aligned} \tag{2.25}$$

Since

$$\phi_i = \sqrt{\frac{2}{\pi}}\cos(ix), \quad \int_0^\pi \phi_i^3\,\mathrm{d}x = 0,$$

this leads to $\langle F_{QQ}(d_{1,i},(0,0))\Phi_i^2,\Phi_i^*\rangle = 0$, so $d_1'(0) = 0$.

Using expression (2.14) in [29], the direction of steady-state bifurcation is subcritical if

$$d_1''(0) = -\frac{\langle F_{QQQ}(d_{1,i},(0,0))\Phi_i^3,\Phi_i^*\rangle + 3\langle F_{QQ}(d_{1,i},(0,0))\Phi_i\theta,\Phi_i^*\rangle}{3\langle F_{dQ}(d_{1,i},(0,0))\Phi_i,\Phi_i^*\rangle} < (>)0,$$

Where θ is the solution of the following problem:

$$F_{QQ}(d_{1,i},(0,0))\Phi_i^2 + F_Q(d_{1,i},(0,0))\theta = 0.$$

After calculation, we have

$$\langle F_{QQQ}(d_{1,i},(0,0))\Phi_i^3,\Phi_i^*\rangle = \frac{4}{\pi^2}(m_i + n_i e_i^*)\int_0^\pi \cos^4(ix)dx = \frac{3}{2\pi}(m_i + n_i e_i^*),$$

where $m_i = -p\eta_i$ and

$$m_i = \tilde{q}_{www}(0,0) + 3\tilde{q}_{wwn}(0,0)e_i + 3\tilde{q}_{wnn}(0,0)e_i^2 + \tilde{q}_{nnn}(0,0)e_i^3 = (3\tilde{q}_{wnn}(0,0) + \tilde{q}_{nnn}(0,0)e_i)\,e_i^2.$$

Let $\theta = (\theta_1,\theta_2)$. Then, it satisfies

$$\begin{cases} d_{1,i}\theta_1'' + \tilde{q}_w(0,0)\theta_1 + \tilde{q}_n(0,0)\theta_2 = -k_i\phi_i^2, & x\in(0,\pi), \\ d_{2,i}\theta_2'' + \tilde{b}_w(0,0)\theta_1 + \tilde{b}_n(0,0)\theta_2 = -r_i\phi_i^2, & x\in(0,\pi), \\ \theta_i'(0) = \theta_i'(\pi) = 0, & i = 1,2. \end{cases} \tag{2.26}$$

Integrate (2.26) over $[0,\pi]$ and solve the binary linear system to get

$$\int_0^\pi \theta_1 dx = \frac{r_i\tilde{q}_n(0,0) - k_i\tilde{b}_n(0,0)}{\tilde{q}_w(0,0)\tilde{b}_n(0,0) - \tilde{q}_n(0,0)\tilde{b}_w(0,0)} = \frac{-pbr_i}{\mathrm{Det}J}, \tag{2.27}$$

$$\int_0^\pi \theta_2 dx = \frac{k_i\tilde{q}_n(0,0) - r_i\tilde{b}_n(0,0)}{\tilde{q}_w(0,0)\tilde{b}_n(0,0) - \tilde{q}_n(0,0)\tilde{b}_w(0,0)} = \frac{r_i}{\mathrm{Det}J}. \tag{2.28}$$

A direct calculation yields

$$\langle F_{QQ}(d_{1,i},(0,0))\Phi_i\theta,\Phi_i^*\rangle = I_1\int_0^\pi \theta_1\phi_i^2 dx + I_2\int_0^\pi \theta_2\phi_i^2 dx,$$

where

$$I_1 = \tilde{q}_{ww}(0,0) + \tilde{q}_{wn}(0,0)e_i + \left(\tilde{b}_{ww}(0,0) + \tilde{b}_{wn}(0,0)e_i\right)e_i^*,$$
$$I_2 = \tilde{q}_{wn}(0,0) + \tilde{q}_{nn}(0,0)e_i + \left(\tilde{b}_{wn}(0,0) + \tilde{b}_{nn}(0,0)e_i\right)e_i^*.$$

Based on the values of e_i, e_i^*, we have

$$I_1 = e_i\left(e_i^* - p\right)\tilde{b}_{nn}(0,0) = \frac{pn^{*3}\left(\sigma n^*+2\right)\left(1+\sigma n^*+n^{*2}\right)\left(d_2\lambda_i+b\right)}{\left[\left(d_2\lambda_i-b\right)\left(1+\sigma n^*+n^{*2}\right)^2 + vn^*\left(\sigma n^*+2\right)\right]^2}, \tag{2.29}$$

$$\begin{aligned} I_2 &= \left(e_i^*-p\right)\left(\tilde{b}_{wn}(0,0)+\tilde{b}_{nn}(0,0)e_i\right) \\ &= -\frac{p(d_2\lambda_i-b)\cdot n^*(\sigma n^*+2)\left[(d_2\lambda_i-b)(1+\sigma n^*+n^{*2}) + w^*n^*(\sigma n^*+2)\right]}{\left[(d_2\lambda_i-b)(1+\sigma n^*+n^{*2}) + w^*n^*(\sigma n^*+2)\right]^2} \\ &\quad - \frac{p(d_2\lambda_i-b)\cdot n^{*2}(1+\sigma n^*+n^{*2})\left(b\sigma + b\sigma n^{*2} + 4bn^*\right)}{\left[(d_2\lambda_i-b)(1+\sigma n^*+n^{*2}) + w^*n^*(\sigma n^*+2)\right]^2}. \end{aligned} \tag{2.30}$$

Based on the above calculation process, we obtain the following integral results:

$$\int_0^\pi \theta_1\phi_i^2 dx \quad \text{and} \quad \int_0^\pi \theta_2\phi_i^2 dx.$$

Multiply (2.26) by ϕ_i^2, and note that

$$\int_0^\pi \phi_i^4 dx = \frac{4}{\pi^4}\int_0^\pi \cos^4(ix)dx = \frac{3}{2\pi}.$$

We get

$$d_{1,i}\int_0^\pi \theta_1''\phi_i^2 \mathrm{d}x + \tilde{q}_w(0,0)\int_0^\pi \theta_1\phi_i^2\mathrm{d}x + \tilde{q}_n(0,0)\int_0^\pi \theta_2\phi_i^2\mathrm{d}x = -\frac{3}{2\pi}k_i, \tag{2.31}$$

and

$$d_2\int_0^\pi \theta_2''\phi_i^2 \mathrm{d}x + \tilde{b}_w(0,0)\int_0^\pi \theta_1\phi_i^2\mathrm{d}x + \tilde{b}_n(0,0)\int_0^\pi \theta_2\phi_i^2\mathrm{d}x = -\frac{3}{2\pi}r_i. \tag{2.32}$$

Integrating by parts over $[0,\pi]$, we have

$$\int_0^\pi \theta_j''\phi_i^2\mathrm{d}x = \frac{4i^2}{\pi}\int_0^\pi \theta_j(1-\pi\phi_i^2)\mathrm{d}x, \quad j=1,2. \tag{2.33}$$

Substitute (2.27), and (2.33) into (2.31) and (2.32), and rearrange to get

$$(\tilde{q}_w(0,0) - 4i^2 d_{1,i})\int_0^\pi \theta_1\phi_i^2\mathrm{d}x + \tilde{q}_n(0,0)\int_0^\pi \theta_2\phi_i^2\mathrm{d}x = -\frac{3}{2\pi}k_i + \frac{4i^2 pbr_i}{\pi \mathrm{Det}J}d_{1,i},$$

and

$$\tilde{b}_w(0,0)\int_0^\pi \theta_1\phi_i^2 \mathrm{d}x + (\tilde{b}_n(0,0) - 4i^2d_2)\int_0^\pi \theta_2\phi_i^2 \mathrm{d}x = -\frac{3}{2\pi}r_i - \frac{4i^2r_i}{\pi \mathrm{Det}J}d_2.$$

Solve the above binary linear system:

$$\beta_1 \triangleq \int_0^\pi \theta_1\phi_i^2 \mathrm{d}x = \frac{-\frac{3}{2\pi}(r_i\tilde{q}_n + 4i^2k_id_2 - k_i\tilde{b}_n) - \frac{4i^2r_i}{\pi \mathrm{Det}J}(d_2\tilde{q}_n - 4i^2pbd_{1,i}d_2 + pbd_{1,i}\tilde{b}_n)}{q_n\tilde{b}_w - (-4i^2d_{1,i} + \tilde{q}_w)(-4i^2d_2 + \tilde{b}_n)},$$

$$\beta_2 \triangleq \int_0^\pi \theta_2\phi_i^2 \mathrm{d}x = \frac{-\frac{3}{2\pi}(k_i\tilde{b}_w + 4i^2d_{1,i}r_i - r_i\tilde{q}_w) + \frac{4i^2r_i}{\pi \mathrm{Det}J}(pbd_{1,i}\tilde{b}_w - 4i^2d_{1,i}d_2 + d_2\tilde{q}_w)}{q_n\tilde{b}_w - (-4i^2d_{1,i} + \tilde{q}_w)(-4i^2d_2 + \tilde{b}_n)}.$$

By the expression of $d_{1,i}$, we find

$$\begin{aligned}&\tilde{q}_n\tilde{b}_w - (4i^2d_1, i + \tilde{q}_w)(-4i^2d_2 + \tilde{b}_n)\\ &= (4i^2d_1 + 1)\left(\frac{b(\sigma n^* + 2)}{1 + \sigma n^* + n^{*2}} - b\right) + \frac{n^{*2}}{1 + \sigma n^* + n^{*2}}(4i^2d_2 - pb) - 16i^4d_1d_2. \end{aligned} \tag{2.34}$$

In summary,

$$d_1''(0) = \frac{n_i\left(e_i^* - p\right) + 2\pi\left(C_1\beta_1 + C_2\beta_2\right)}{2\pi\lambda_i}.$$

We obtain the following theorem.

Theorem 2.16. *If $d_1''(0) > 0$, then the bifurcation obtained from $(d_{1,i}, (0,0))$ in Theorem 2.11 is supercritical. If $d_1''(0) < 0$, then the bifurcation obtained from $(d_{1,i}, (0,0))$ in Theorem 2.11 is subcritical.*

3. Numerical simulations

In this study, the two-dimensional spatial domain is discretized using the second-order central finite difference method on a uniform 200×200 grid with a spatial step size of $h = 1$. The Laplacian operator is approximated via the five-point central difference scheme, subject to Neumann boundary conditions. For temporal integration, the explicit forward Euler method is employed with a time step size of $\tau = 0.001$, and a total simulation time of 100 is adopted to ensure the full evolution of Turing patterns to a steady state. The homogeneous steady state of the system is solved by the built-in function fsolve; a multi-initial-point strategy is implemented, and a convergence tolerance of 10^{-6} is set to guarantee the robustness of the solution. Systematic tests are conducted on multiple parameter sets to verify the correctness of the previous theoretical analyses, and further reveal the dynamic behavioral characteristics of the system across different parameter spaces and their ecological implications.

In the first set of numerical experiments, the selected parameters are: $d_1 = 50$, $d_2 = 0.1$, $b = 1.5$, $a = 8.5$, $\sigma = 0.4 < \sigma_0$, *and* $p = 4$. For this configuration, the conditions $d_2\lambda_1 < \frac{b(1-n^{*2})}{1+\sigma n^*+n^{*2}}$, and $d_1 > \widehat{d_1}$ are satisfied. According to Theorem 2.7(ii), the equilibrium point (w^*, n^*) is unstable. The numerical simulation results (see Figure 1) clearly show that the system cannot maintain equilibrium under these parameters, with state variables exhibiting divergent or sustained oscillatory behavior. As illustrated in the figure, even when minor perturbations are applied near the equilibrium point, the

system rapidly deviates from its original state, displaying significant instability characteristics. This verifies the threshold conditions for Turing instability derived from the theoretical analysis and reveals that under conditions of low competition intensity and high water diffusion, the system may transition into pattern formation or oscillatory states.

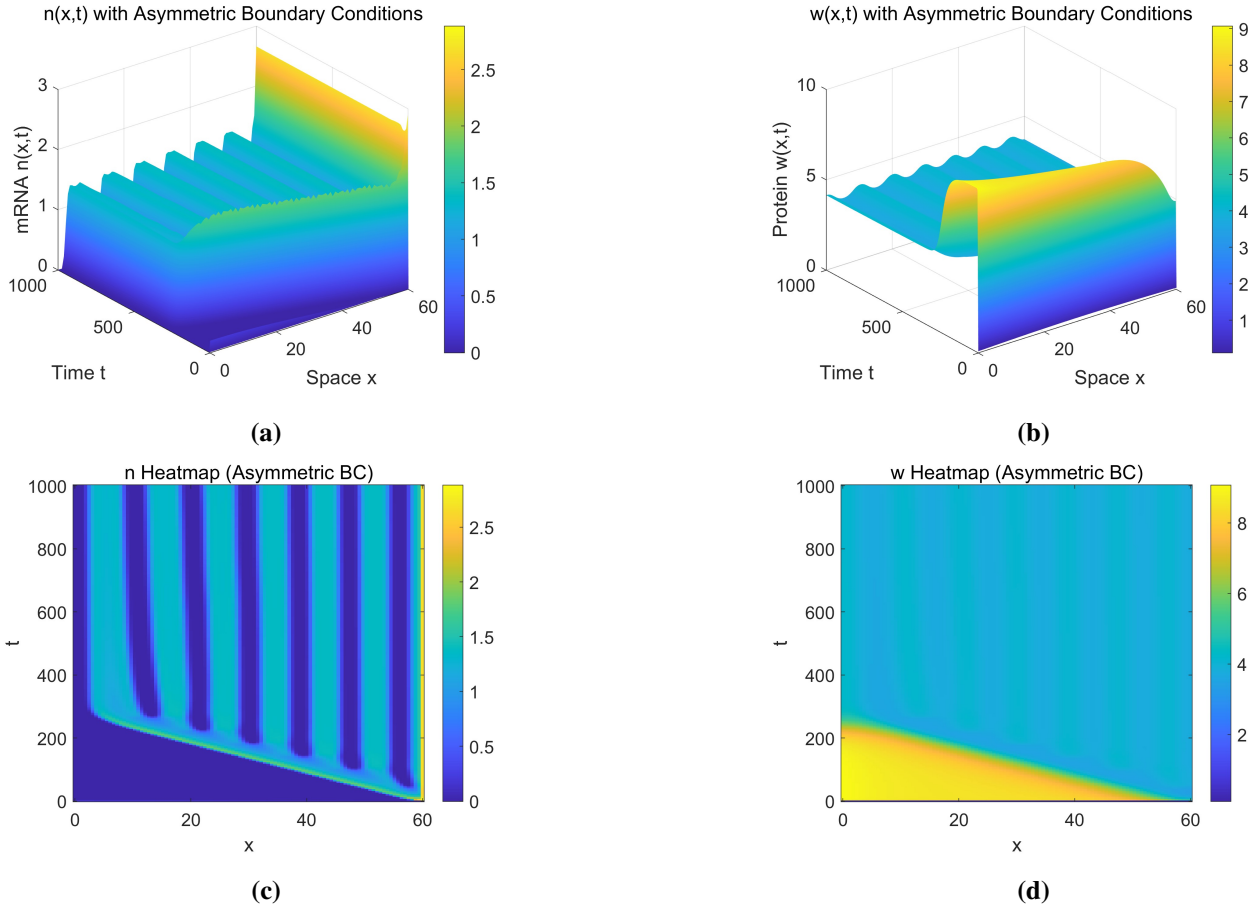

Figure 1. When parameters are set as $d_1 = 50, d_2 = 0.1, b = 1.5, a = 8.5, \sigma = 0.4, and\ p = 4$, the equilibrium state (w^*, n^*) of system 1.5 is unstable, and Turing instability may occur.

In the second set of numerical experiments, some parameters are adjusted: $d_1 = 5$, $d_2 = 0.05$, $b = 1.5$, $a = 9$, $\sigma = 3 > \sigma_0$, *and* $p = 6$. These parameters satisfy $\sigma > \sigma_0$ and $0 < \frac{d_1}{d_2} < z_2$. According to Theorem 2.4, the positive equilibrium (w^*, n^*) is locally asymptotically stable under these conditions. The numerical simulation results (see Figure 2) visually demonstrate that after being subjected to minor perturbations, the state variables of the system converge to the equilibrium point over time, thereby confirming the correctness of the theoretical analysis. Specifically, the evolutionary trajectories of w and n in the figure exhibit clear damped oscillatory processes, eventually stabilizing at steady-state values. This indicates that under these parameter conditions, the vegetation-water system possesses strong self-recovery capabilities and stability maintenance mechanisms, allowing the ecosystem to effectively return to equilibrium under external disturbances.

Next, we analyze the patterns generated by Turing instability in this system within the time interval $[0, 100]$. Figure 3 illustrates the evolution of the vegetation biomass spatial distribution at

$t = 0s, 20s, 50s, 80s, 100s$ when the steady-state solutions w^* and n^* are disturbed. The sequence of snapshots demonstrates a complete morphological evolution: from "random initial perturbations" to "ordered nucleation" to "mature pattern stabilization". Among them, the blue regions represent low-humidity areas, and the red regions represent high-humidity areas. At $t = 0s$, the system starts with uniform random disturbances, and no diffusion reaction has occurred yet, so the spatial distribution is in disordered random motion. At $t = 20s$, the disturbances are amplified, and regular spot structures gradually form, which is a manifestation of system instability. At $t = 50s$, the patterns converge toward regular spotted formations, with spatial density stabilizing. At $t = 80s$, the spotted structures become more distinct and orderly, eventually developing into steady vegetation patterns with pronounced spatial periodicity.

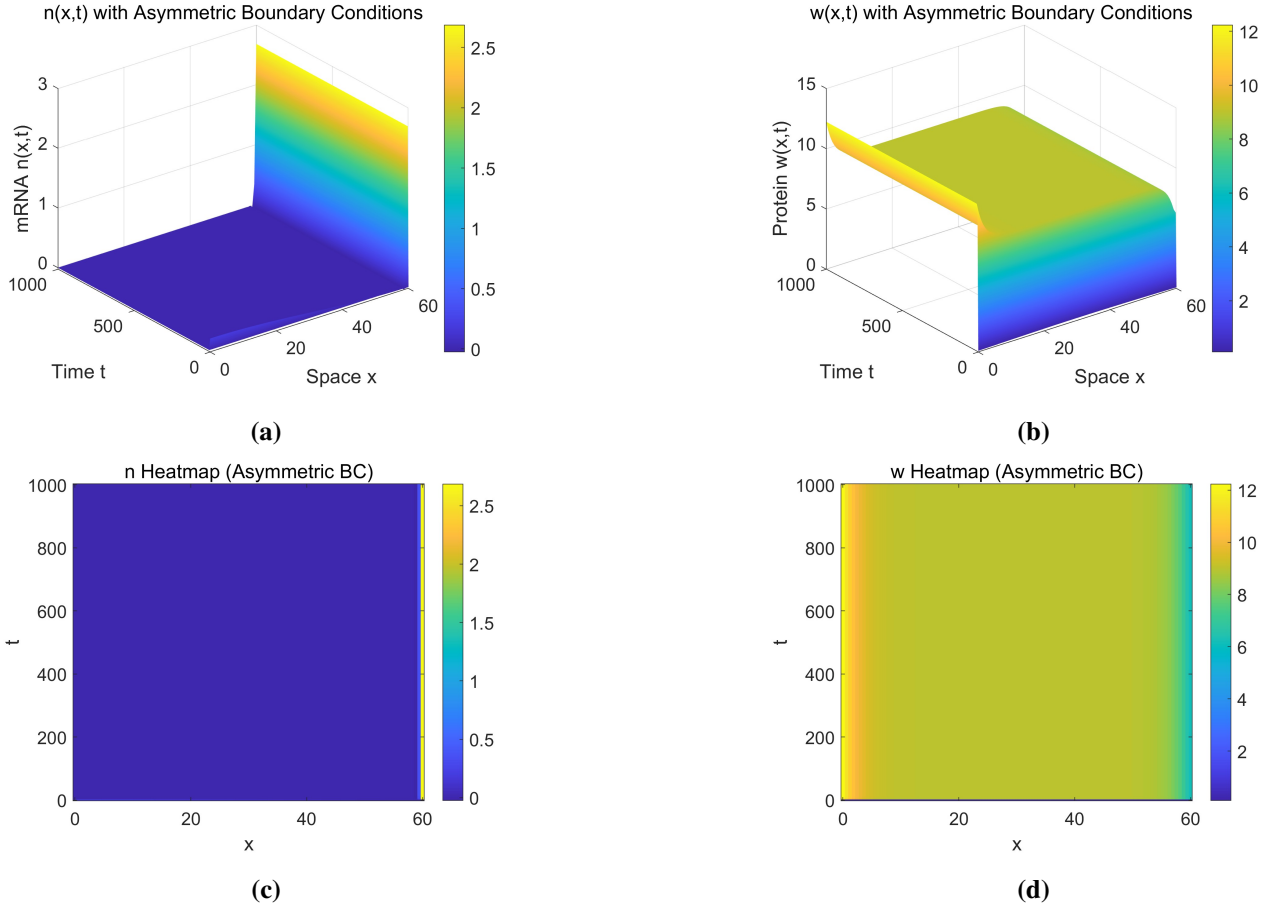

Figure 2. When parameters are set as $d_1 = 5, d_2 = 0.05, b = 1.5, a = 9, \sigma = 3, and\ p = 6$, the equilibrium state (w^*, n^*) of system 1.5 is locally asymptotically stable.

This section focuses on discussing the influence of parameter variations on vegetation pattern morphology. We systematically analyze five key parameters to investigate the intrinsic relationship between vegetation pattern structure and parameter changes.

The first parameter examined is the water diffusion coefficient d_1. Figure 4 illustrates the steady-state spatial distribution of vegetation and its dynamic evolution under different values of d_1. Numerical simulation results show that when d_1 is relatively small, regular high-density spots appear (Figure 4(a)).

A small d_1 indicates slow water diffusion, which restricts effective water absorption and utilization to only localized vegetation patches, resulting in spatially separated and relatively uniformly distributed vegetation clusters. However, when the value of d_1 increases, the system 1.5 exhibits high-density mixed patterns, characterized by a coexistence of stripe and spot structures, as shown in Figure 4(b). If d_1 is further increased, the pattern gradually transitions from spots to stripes (Figure 4(c)). Finally, regular stripe patterns emerge (Figure 4(d)).

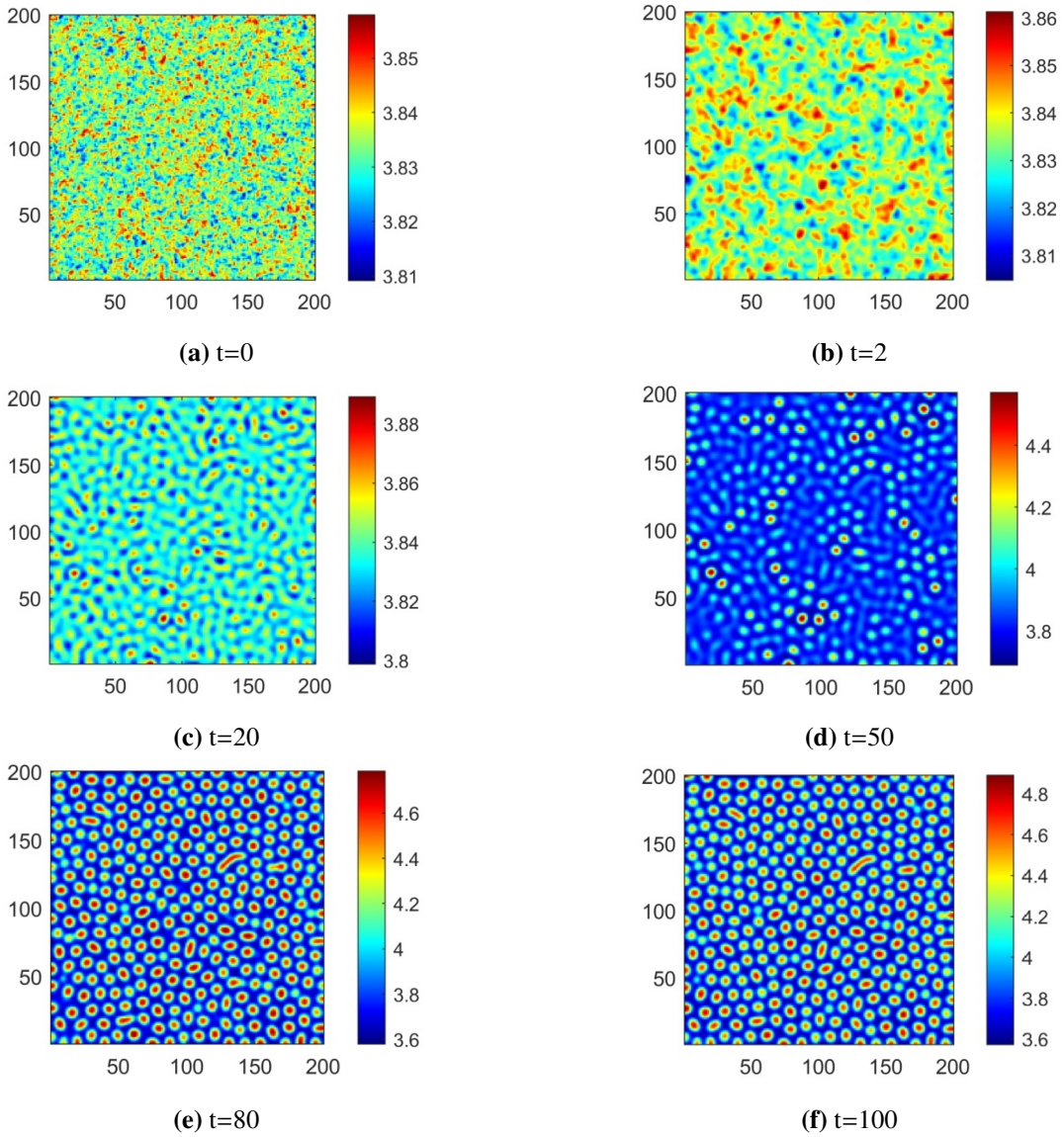

(a) t=0 **(b)** t=2

(c) t=20 **(d)** t=50

(e) t=80 **(f)** t=100

Figure 3. Evolution process of vegetation at $t = 0s, 2s, 20s, 50s, 80s, 100s$ under other parameters.

From the evolution of vegetation patterns, it can be observed that as d_1 increases, vegetation density gradually decreases and spatial distribution becomes more dispersed. Enhanced water diffusion expands areas of high moisture, confining vegetation to isolated small regions, leading to a reduction in overall vegetation density. d_1 corresponds to the hydrological properties of soil: A low d_1

value is associated with soils of high water retention capacity, which tend to form stable, high-density spot vegetation patterns-an ideal vegetation structure for windbreak and sand fixation in semi-arid regions; while a high d_1 value corresponds to permeable sandy soils, where vegetation exhibits a striped distribution with lower overall density, a typical vegetation characteristic of desertified land. This result provides direct guidance for ecological restoration in arid areas: in regions with high water-retention soils, spot planting can be adopted to cultivate high-density vegetation; in sandy areas, vegetation should be planted in accordance with the striped pattern. Meanwhile, changes in vegetation pattern morphology can be used to intuitively assess soil hydrological function and desertification degree, providing a basis for desertification monitoring.

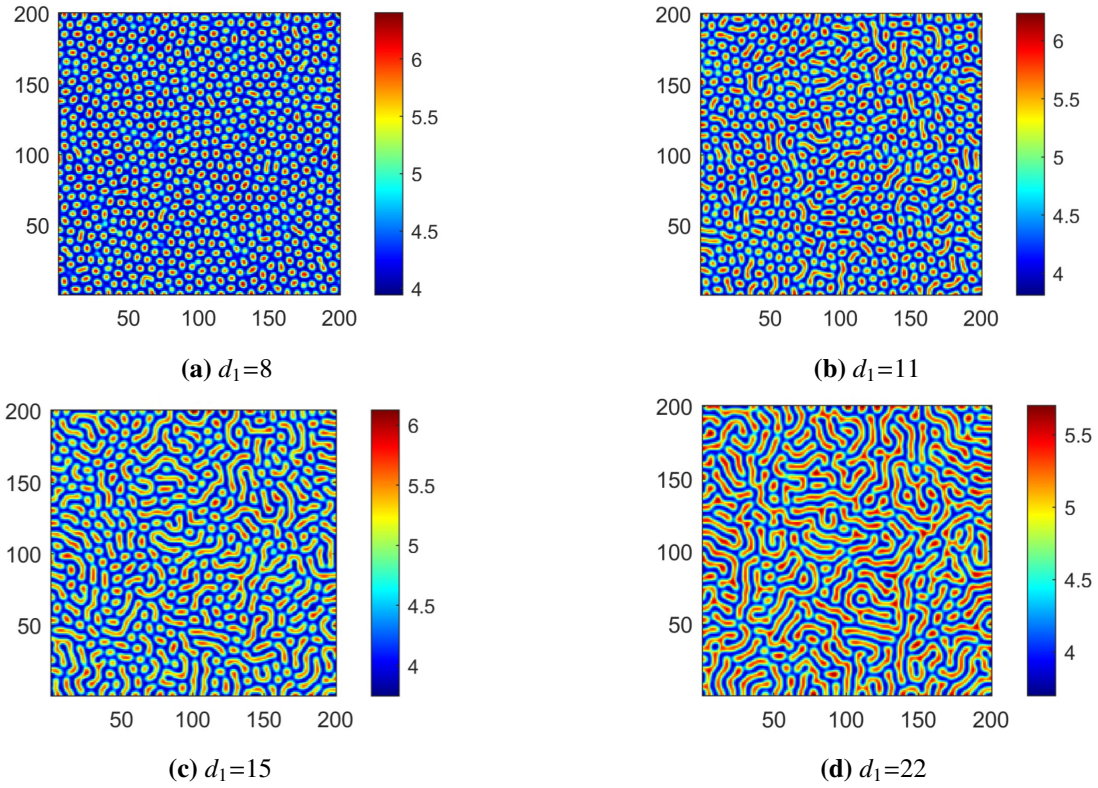

(a) d_1=8 **(b)** d_1=11

(c) d_1=15 **(d)** d_1=22

Figure 4. Evolution process of vegetation patterns when $d_2 = 0.7$, $a = 9$, $p = 6$, $\sigma = 0.5$, $b = 1.5$, and $d_1 = 8, 11, 15, 22$.

The second parameter under discussion is the internal competition of vegetation: σ. In Figure 5, the patterns change from spots to stripes. When σ is small, the vegetation shows a discrete "clustered" distribution. At this time, the internal competition is weak, and the pattern formation mechanism dominated by "short-range activation and long-range inhibition" leads to the appearance of regular high-density spots (Figure 5(a)). When σ is small, a mixed structure of spots and stripes appears. The enhancement of internal competition makes the local vegetation start to expand spatially. However, when the value of σ increases, system 1.5 exhibits high-density mixed-mode stripes and spots, with striped patterns becoming the main body, as shown in Figure 5(b). If σ is further increased, the internal competition is further intensified, and the spatial expansion ability of vegetation exceeds the restriction

of "long-range inhibition", gradually changing from spots to stripes (Figure 5(c)). Finally, a regular stripe pattern appears (Figure 5(d)).

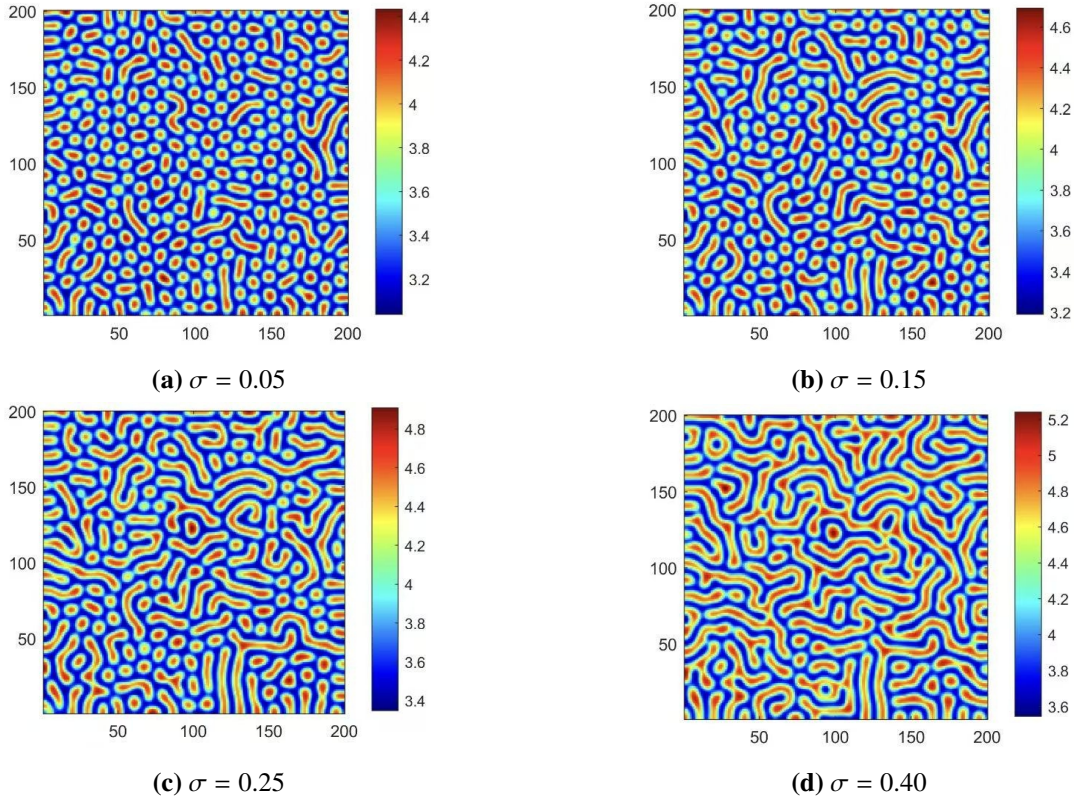

(a) $\sigma = 0.05$ **(b)** $\sigma = 0.15$

(c) $\sigma = 0.25$ **(d)** $\sigma = 0.40$

Figure 5. Evolution process of vegetation patterns when $d_1 = 25$, $d_2 = 0.5$, $p = 6$, $a = 9$, $b = 1.5$, and $\sigma = 0.05, 0.15, 0.25, 0.4$.

When the resource competition between vegetation is weak, the role of "activators" is more prominent, forming discrete spots, each of which is a vegetation cluster, and the clusters maintain intervals through "long-range inhibition". When the resource competition between vegetation is strong, the role of "inhibitors" is amplified, and the spots connect into stripes. A low σ indicates a low vegetation population density and weak intraspecific competition, which tends to form scattered, high-density spot vegetation clusters. This pattern allows vegetation to fully utilize local water resources and is a typical state in the early stage of natural vegetation restoration in semi-arid regions. A high σ represents a high population density and intense intraspecific competition, resulting in a more uniform overall distribution of vegetation, which is a sign of a well-developed and stable vegetation community. This result demonstrates that in the early stage of vegetation restoration, we can reduce intraspecific competition by controlling planting density, promote the formation of spot vegetation clusters, and accelerate the stability of the ecosystem; in mature vegetation areas, we can regulate the competition intensity through moderate thinning to avoid vegetation degradation caused by excessive competition. Meanwhile, the morphology of vegetation patterns can be used to intuitively judge the population competition status and community development stage, providing a basis for ecosystem health assessment.

As a key indicator of water input in ecosystems, the rainfall rate a, serves as an important driving factor influencing the spatial distribution patterns of vegetation. Figure 6 systematically illustrates the steady-state vegetation pattern morphology formed by the system under different rainfall rates a, clearly revealing the dynamic transition process from stripe patterns to spotted patterns. When the rainfall rate a is at a relatively low level, a stripe patterns appear (Figure 6(a)). If a is further increased, the vegetation distribution displays a mixed stripe-spot pattern (as shown in Figure 6(b)). Under such conditions, water supply is limited, leading vegetation to form adaptive spatial configurations in response to restricted moisture availability. Through localized aggregation, vegetation reduces water competition pressure, while gap patterns (Figure 6(c)) gradually emerge. When a is progressively increased further, perfect gap patterns (Figure 6(d)) eventually develop.

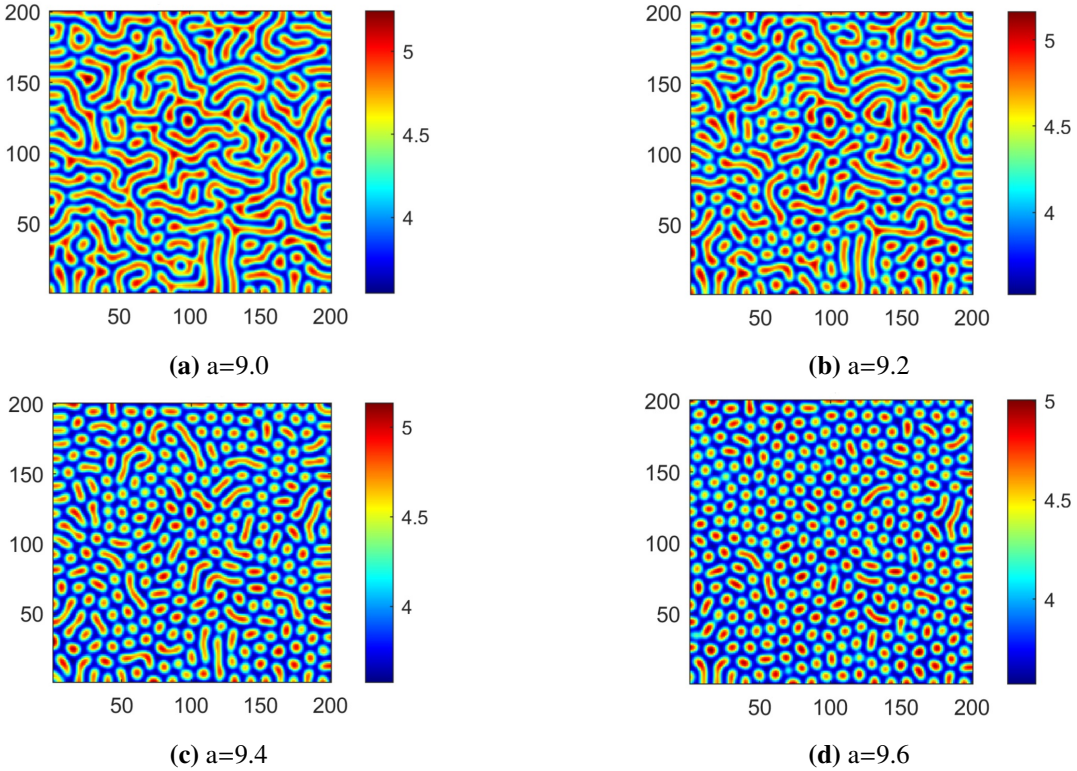

(a) a=9.0 **(b)** a=9.2

(c) a=9.4 **(d)** a=9.6

Figure 6. Vegetation Patterns in system 1.5 given $p = 6$, $b = 1.5$, $sigma = 0.4$, $d_1 = 25$, $d_2 = 0.5$, and $a = 9.0, 9.2, 9.4, 9.6$.

These results clearly demonstrate that, within a specific parameter range, the rainfall rate a is positively correlated with vegetation density. The increase in water supply effectively promotes vegetation coverage and overall density. The above experimental results indicate that under low rainfall rates, vegetation forms striped patterns to conserve water, while under high rainfall rates, it develops into high-density spot patterns to fully utilize water resources. This evolutionary process is highly consistent with the vegetation gradient from desert steppe to typical steppe in China's arid regions, verifying the ecological rationality of the model. This result provides direct guidance for ecological restoration in arid areas: In desertified regions with scarce rainfall, strip planting can be adopted in accordance with the striped pattern to reduce water competition and improve vegetation

survival rate; in regions with relatively sufficient rainfall, spot planting is used to cultivate high-density spot vegetation, enhancing the efficiency of windbreak and sand fixation and the stability of the ecosystem. Meanwhile, vegetation patterns can be used to assess regional water supply status and ecosystem health.

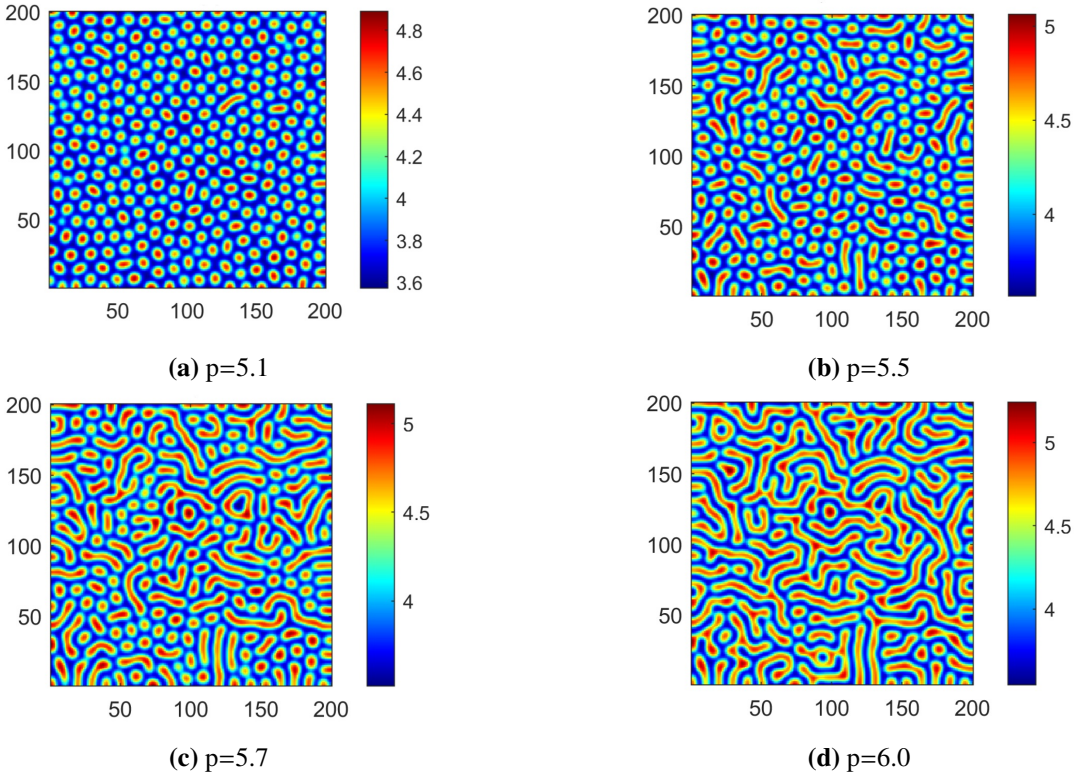

(a) p=5.1 **(b)** p=5.5

(c) p=5.7 **(d)** p=6.0

Figure 7. Evolution process of vegetation patterns when $d_1 = 25$, $d_2 = 0.5$, $\sigma = 6$, $a = 0.4$, $b = 1.5$, and $p = 5.1, 5.5, 5.7, 6.0$.

Finally, we investigated the regulatory effect of parameter p on the evolution of two-dimensional vegetation patterns. Figure 7 fully illustrates the complete dynamic transition of vegetation pattern morphology from discrete spotted structures to continuous striped structures as the value of p increases gradually. Specifically, parameter p in this model characterizes the strength of the nonlinear feedback between vegetation and water: when p is small, the coupling feedback between vegetation and water is weak, and the system, dominated by the core mechanism of "short-range activation and long-range inhibition", forms spatially separated, uniformly distributed high-density spot patterns, where vegetation fully utilizes local water resources through localized aggregation. As p continues to increase, the nonlinear feedback between vegetation and water is continuously enhanced, the spatial expansion capacity of vegetation is gradually improved, the originally independent spots gradually connect and merge, and the pattern morphology transitions from spots to stripes. When p reaches a high level, the dominance of the feedback effect is further highlighted, eventually forming a regular, continuous banded spatial distribution pattern, where vegetation extends in strips along water-enriched zones to maximize the utilization of regional water resources.

A low p corresponds to a degraded ecosystem with a small vegetation population size and low

water use efficiency, which tends to form scattered spot vegetation clusters and is a typical state in the early stage of vegetation restoration in arid areas; a high p corresponds to a mature community with strong vegetation-water coupling and a stable ecosystem, and the formed banded pattern is an ideal vegetation configuration for windbreak, sand fixation, and desertification resistance in semi-arid areas. This indicates that in the early stage of vegetation restoration, the feedback between vegetation and water can be enhanced through artificial water supplementation, optimization of planting structure, and other measures to promote the evolution of vegetation from spot to stripe patterns and accelerate the stability of the ecosystem; in desertification control, artificial vegetation sand barriers can be constructed in accordance with the banded pattern under high p to improve the efficiency of windbreak and sand fixation.

In this chapter, the numerical simulations comprehensively verify the stability and Turing instability criteria obtained from the preceding theoretical analysis, clearly reveal the regulatory effects of the water diffusion coefficient d_1, intraspecific competition coefficient *sigma*, precipitation rate a, and feedback intensity parameter p on the evolution of vegetation patterns, elucidate the dynamic transition laws of patterns from spot-like to stripe-like structures and vice versa, and clarify the ecosystem transformations induced by each parameter. These findings provide theoretical support and practical guidance for ecosystem management and desertification control.

4. Conclusions

This study focuses on a vegetation-water system that integrates saturated water uptake and intraspecific competition, uncovering core dynamic rules of arid ecosystems through multidimensional analysis. Theoretically, we elucidated the distinct stability characteristics of the positive equilibrium states: the low-density equilibrium is inherently unstable, while the other positive equilibrium exhibits Turing instability. This instability is jointly regulated by the relative magnitudes of the vegetation and water diffusion coefficients-specifically, pattern formation is triggered when the vegetation diffusion coefficient is sufficiently small or the water diffusion coefficient is sufficiently large.

Based on a priori estimates derived from the maximum principle, we defined the boundary of non-negative steady-state solutions for the model, laying a foundation for subsequent bifurcation analyses. Through qualitative analysis of steady-state bifurcations at simple and double eigenvalues, we further identified dynamic criteria for bifurcation directions and clarify the pattern evolution logic of the system under parameter perturbations. Numerical simulation results intuitively demonstrate the vegetation pattern evolution process under different parameter combinations: As the water diffusion coefficient and intraspecific competition coefficient increase, vegetation distribution gradually transitions from compact spot-like structures to stripe-like structures; conversely, an increase in the precipitation parameter drives a reverse pattern shift, contracting stripe-like structures back into discrete spot-like distributions.

These findings not only refine the theoretical framework for modeling vegetation-water interactions, but also provide a new analytical perspective for understanding pattern formation mechanisms in arid ecosystems. The stability criteria and bifurcation analysis methods developed in this study can serve as theoretical tools for quantifying vegetation resilience and predicting risks of ecological degradation. Furthermore, the revealed rules of pattern evolution driven by key parameters

offer scientifically grounded insights for water resource management and vegetation restoration strategies in arid regions.

Use of AI tools declaration

All research content, academic viewpoints, data arguments, and core conclusions presented in this paper were independently completed by the authors. AI tools served only as auxiliary means and did not participate in core academic processes such as research design, data processing, or conclusion derivation. The authors strictly adhered to academic integrity norms and the relevant requirements of the journal.

Acknowledgments

This work was supported by the National Natural Science Foundation of China (No.12326417); Shaanxi Province Natural Science Foundation Research Project (N2024JCYBMS072); Key Project of Shaanxi Province Foreign Expert Service Plan (2024WZ-YBXM01); Provincial and Ministerial-Level Special Project (G20241239); Xi'an Science and Technology Plan Project (No.25ZQRC00026); Education and Teaching Reform Project of Shaanxi Province (No.26BY078); Xi'an Technological University Graduate Education and Teaching Reform Project (No.XAGDYJ250107).

Conflict of interest

The authors declare there is no conflict of interest.

References

1. L. I. M. Linhares, P. R. Mutti, B. M. Funatsu, V. Dubreuil, B. G. Bezerra, A. S. F. S. Martins, et al., Areas susceptible to desertification in brazil: an approach based on the frequency of annual aridity classes, *Atmos. Res.*, **329** (2026), 108477. https://doi.org/10.1016/j.atmosres.2025.108477
2. H. K. Ishaq, E. Grilli, G. Busico, M. Mastrocicco, F. A. Rutigliano, M. Bjil, et al., Enhancing ecosystem services by introducing multifunctional land use management in a semiarid pastoral system in portugal, *Total Environ. Adv.*, **16** (2025), 200138. https://doi.org/10.1016/j.teadva.2025.200138
3. Z. Yu, L. Jiang, Y. Liu, Quantifying and separating the impact of climate change and human activities on vegetation in transboundary regions, *Environ. Sustainability Indic.*, **28** (2025), 100943. https://doi.org/10.1016/j.indic.2025.100943
4. Y. Altowaijri, S. M. Ahmad, P. Mandal, Effect of short- and long-term seasonal climate change variations on the stability of a vegetated slope in London clay, *Int. J. Geomech.*, **25** (2025), 1–10. https://doi.org/10.1061/IJGNAI.GMENG-10978
5. C. Li, Z. Jin, C. Jiang, Y. Shen, R. Wang, J. Peng, How topographic and pedological factors affect vegetation responses to drought: a study from the qinling mountains, China, *Catena*, **260** (2025), 109470. https://doi.org/10.1016/j.catena.2025.109470

6. Y. Zhang, Z. Wang, X. Shi, P. Sun, P. Xiao, J. Xu, et al., Impacts of climate change and vegetation greening driven by natural and anthropogenic factors on carbon sink in chinese loess plateau after ecological restoration, *Catena*, **258** (2025), 109310. https://doi.org/10.1016/j.catena.2025.109310
7. J. Solon, Anthropogenic disturbance and vegetation diversity in agricultural landscapes, *Landscape Urban Plann.*, **31** (1995), 171–180. https://doi.org/10.1016/0169-2046(94)01043-8
8. T. Bao, H. Li, Y. Hao, M. T. Harrison, K. Liu, G. Ali, Anthropogenic and natural influence on vegetation ecosystems from 1982 to 2023, *Environ. Res. Lett.*, **20** (2025), 094051. https://doi.org/10.1088/1748-9326/adf980
9. G. Guo, X. Zou, Y. Zhang, The dual effects of climate change and human activities on the spatiotemporal vegetation dynamics in the inner mongolia plateau from 1982 to 2022, *Land*, **14** (2025), 1559. https://doi.org/10.3390/land14081559
10. M. P. Carneiro, P. F. Gabetto, F. M. Costa, V. Meneghini, J. E. Santos de Sousa, G. A. G. Pereira, et al., Biochar-mediated improvements in soil health in drylands: a bibliometric review of the potential and mechanisms for combating desertification and climate change, *J. Arid. Environ.*, **232** (2026), 105490. https://doi.org/10.1016/j.jaridenv.2025.105490
11. A. Mavrakis, C. Papavasileiou, L. Salvati, Towards (un)sustainable urban growth? industrial development, land-use, soil depletion and climate aridity in a greek agro-forest area, *J. Arid. Environ.*, **121** (2015), 1–6. https://doi.org/10.1016/j.jaridenv.2015.05.003
12. E. Meron, Pattern formation-a missing link in the study of ecosystem response to environmental changes, *Math. Biosci.*, **271** (2016), 1–18. https://doi.org/10.1016/j.mbs.2015.10.015
13. S. Mangla, R. L. Sheley, J. J. James, S. R. Radosevich, Intra and interspecific competition among invasive and native species during early stages of plant growth, *Plant Ecol.*, **212** (2011), 531–542. https://doi.org/10.1007/s11258-011-9909-z
14. D. Donzelli, C. De Michele, R. J. Scholes, Competition between trees and grasses for both soil water and mineral nitrogen in dry savannas, *J. Theor. Biol.*, **332** (2013), 181–190. https://doi.org/10.1016/j.jtbi.2013.04.003
15. Z. Ying, J. Liao, Y. Liu, S. Wang, H. Lu, L. Ma, et al., Modelling tree-grass coexistence in water-limited ecosystems, *Ecol. Modell.*, **360** (2017), 387–398. https://doi.org/10.1016/j.ecolmodel.2017.07.014
16. R. Lefever, O. Lejeune, On the origin of tiger bush, *Bull. Math. Biol.*, **59** (1997), 263–294. https://doi.org/10.1007/BF02462004
17. M. Tlidi, R. Lefever, A. Vladimirov, On vegetation clustering, localized bare soil spots and fairy circles, in *Dissipative Solitons: From Optics to Biology and Medicine* , **751** (2008), 1–22. https://doi.org/10.1007/978-3-540-78217-9_15
18. C. A. Klausmeier, Regular and irregular patterns in semiarid vegetation, *Science*, **284** (1999), 1826–1828. https://doi.org/10.1126/science.284.5421.1826
19. C. E. Tarnita, J. A. Bonachela, E. Sheffer, J. A. Guyton, T. C. Coverdale, R. A. Long, et al., A theoretical foundation for multi-scale regular vegetation patterns, *Nature*, **541** (2017), 398–401. https://doi.org/10.1038/nature20801

20. L. Li, J. Cao, X. Bao, Pattern dynamics of vegetation growth with saturated water absorption, *Front. Phys.*, **9** (2021), 721115. https://doi.org/10.3389/fphy.2021.721115
21. L. Li, F. Wang, L. Hou, Rich dynamics of a vegetation-water system with the hydrotropism effect, *Front. Phys.*, **10** (2023), 1084142. https://doi.org/10.3389/fphy.2022.1084142
22. P. Zhang, K. Wu, Turing instability of the periodic solutions for a vegetation-water model with cross-diffusion, *J. Math. Anal. Appl.*, **553** (2026), 129877. https://doi.org/10.1016/j.jmaa.2025.129877
23. Z. Xiong, Q. Zhang, T. Kang, Bifurcation and stability analysis of a cross-diffusion vegetation-water model with mixed delays, *Math. Methods Appl. Sci.*, **44** (2021), 9976–9986. https://doi.org/10.1002/mma.7384
24. G. Guo, Q. Qin, D. Pang, Y. Su, Positive steady-state solutions for a vegetation–water model with saturated water absorption, *Commun. Nonlinear Sci. Numer. Simul.*, **131** (2024), 107802. https://doi.org/10.1016/j.cnsns.2023.107802
25. X. Wang, G. Zhang, Vegetation pattern formation in seminal systems due to internal competition reaction between plants, *J. Theor. Biol.*, **458** (2018), 10–14. https://doi.org/10.1016/j.jtbi.2018.08.043
26. L. Eigentler, Intraspecific competition in models for vegetation patterns: Decrease in resilience to aridity and facilitation of species coexistence, *Ecol. Complexity*, **42** (2020), 100835 https://doi.org/10.1016/j.ecocom.2020.100835
27. Y. Dai, Y. Zhao, B. Sang, Four limit cycles in a predator–prey system of leslie type with generalized holling type iii functional response, *Nonlinear Anal.:Real World Appl.*, **50** (2019), 218–239. https://doi.org/10.1016/J.NONRWA.2019.04.003
28. Y. Liang, Y. Jia, Stability and Hopf bifurcation of a diffusive plankton model with time-delay and mixed nonlinear functional responses, *Chaos, Solitons Fractals*, **163** (2022), 112533. https://doi.org/10.1016/j.chaos.2022.112533
29. J. Shi, Persistence and bifurcation of degenerate solutions, *J. Funct. Anal.*, **169** (1999), 494–531. https://doi.org/10.1006/jfan.1999.3483
30. M. G. Crandall, P. H. Rabinowitz, Bifurcation, perturbation of simple eigenvalues, and linearized stability, *Arch. Rational Mech. Anal.*, **52** (1973), 161–180. https://doi.org/10.1007/BF00282325
31. J. Shi, X. Wang, On global bifurcation for quasilinear elliptic systems on bounded domains, *J. Differ. Equations*, **246** (2009), 2788–2812. https://doi.org/10.1016/j.jde.2008.09.009
32. J. Pejsachowicz, P. J. Rabinowitz, Degree theory for C^1 fredholm mappings of index 0, *J. Anal. Math.*, **76** (1998), 289–319. https://doi.org/10.1007/BF02786939

Appendix

A. A priori estimates

Proof. Let $w(x_1) = \max_{\Omega} w(x)$. From the first equation of system (1.5) and Lemma 2.9, we obtain

$$a - w(x_1) - \frac{pw(x_1)n^2(x_1)}{1 + \sigma n(x_1) + n(x_1)^2} \geq 0.$$

Thus,

$$w(x) \le w(x_1) \le a. \tag{A.1}$$

Denote $g = d_1 w + p d_2 n$. Then, g satisfies

$$-\Delta g = a - w - pbn. \tag{A.2}$$

Let $g(x_2) = \max_\Omega g(x)$. By Lemma 2.9, we have

$$a - w(x_2) - pbn(x_2) \ge 0.$$

$$n(x_2) \le \frac{a}{pb}. \tag{A.3}$$

From (A.1) and (A.3), we have

$$pd_2 n(x) < g(x) < g(x_2) < ad_1 + \frac{ad_2}{p},$$

which implies

$$n(x) < \frac{ad_1}{pd_2} + \frac{a}{pb}. \tag{A.4}$$

Let $w(x_3) = \min_\Omega w$. By Lemma 2.9, we have

$$a - w(x_3) - \frac{p w(x_3) n^2(x_3)}{1 + \sigma n(x_3) + n(x_3)^2} \le 0.$$

Therefore, according to the upper limit of n in (A.4), we have

$$w(x) \ge w(x_3) \ge w(x_1) \ge w(x_2), \tag{A.5}$$

where

$$w(x_1) = \frac{a}{1 + \dfrac{p n^2(x_3)}{1 + \sigma n(x_3) + n(x_3)^2}}, w(x_2) = \frac{a\left[(pbd_2)^2 + \sigma(pbd_2)(abd_1 + ad_2) + (abd_1 + ad_2)^2\right]}{(pbd_2)^2 + \sigma(pbd_2)(abd_1 + ad_2) + (abd_1 + ad_2)^2(p+1)}.$$

From the second equation of (1.5), we have

$$-\Delta n + \frac{bn}{d_2} \ge 0.$$

By Lemma 2.8, there exists a positive constant C_0, which depends only on b, d_2, and Ω, such that

$$\int_\Omega n dx \le C_0 \inf_\Omega n. \tag{A.6}$$

Integrating the first equation of system (1.5) over Ω, we obtain

$$\int_\Omega \frac{p w n^2}{1 + \sigma n + n^2} dx = \int_\Omega (a - w) dx,$$

note that from the second equation at steady state, we have $\frac{wn^2}{1+\sigma n+n^2} = bn$. Substituting this into the left-hand side yields

$$pb\int_\Omega n dx = \int_\Omega (a-w)dx.$$

Let $\bar{w} = \frac{1}{|\Omega|}\int_\Omega w dx$ denote the spatial average of w. Then, the above equation becomes

$$(a-\bar{w})|\Omega| = pb\int_\Omega n dx \le pbC_0 \inf_\Omega n. \tag{A.7}$$

It can be derived from (A.7) that

$$n(x) \ge \inf_\Omega n \ge \frac{(a-\bar{w})|\Omega|}{pbC_0}. \tag{A.8}$$

The proof is complete. □

B. Proof of Theorem 2.7 and derivation of bifurcation solutions

Proof. According to the Crandall-Rabinowitz bifurcation theorem for simple eigenvalues in [30], $(d_{1,i},(0,0))$ is a bifurcation point if the following conditions are satisfied.
(i) The linear operators F_{d_1}, F_Q, F_{d_1Q} exist and are continuous;
(ii) $\dim\ker F_Q(d_{1,i},(0,0)) = \text{codim}R(F_Q(d_{1,i},(0,0))) = 1$;
(iii) Let $\ker F_Q(d_{1,i},(0,0)) = \text{span}\{\Phi_i\}$. Then, $F_{d_1Q}(d_{1,i},(0,0))\Phi_i \notin R(F_Q(d_{1,i},(0,0)))$.

Recall the following operation:

$$L(d_{1,i}) = F_Q(d_{1,i},(0,0)) = \begin{pmatrix} d_{1,i}\Delta - 1 - \frac{pn^{*2}}{1+\sigma n^*+n^{*2}} & -\frac{pw^*n^*(\sigma n^*+2)}{(1+\sigma n^*+n^{*2})^2} \\ \frac{n^{*2}}{1+\sigma n^*+n^{*2}} & d_2\Delta + \frac{w^*n^*(\sigma n^*+2)}{(1+\sigma n^*+n^{*2})^2} - b \end{pmatrix}, \quad \Delta = \frac{d^2}{dx^2}.$$

Obviously, the linear operators F_{d_1}, F_Q, and F_{d_1Q} are continuous. Through calculation, we obtain

$$\ker L(d_{1,i}) = \text{span}\{\Phi_i\}, \quad \Phi_i = \begin{pmatrix} 1 \\ e_i \end{pmatrix}\phi_i,$$

where

$$e_i = -\frac{n^{*2}(1+\sigma n^*+n^{*2})}{(d_2\lambda_i - b)(1+\sigma n^*+n^{*2}) + w^*n^*(\sigma n^*+2)} < 0, \quad \dim\ker L(d_{1,i}) = 1.$$

The adjoint operator is defined as

$$L^*(d_{1,i}) = \begin{pmatrix} d_1\Delta - 1 - \frac{pn^{*2}}{1+\sigma n^*+n^{*2}} & \frac{n^{*2}}{1+\sigma n^*+n^{*2}} \\ -\frac{pw^*n^*(\sigma n^*+2)}{(1+\sigma n^*+n^{*2})^2} & d_2\Delta + \frac{w^*n^*(\sigma n^*+2)}{(1+\sigma n^*+n^{*2})^2} - b \end{pmatrix}.$$

Similarly,

$$\ker L^*(d_{1,i}) = \text{span}\{\Phi_i^*\}, \quad \Phi_i^* = \begin{pmatrix} 1 \\ e_i^* \end{pmatrix}\phi_i,$$

where

$$e_i^* = \frac{pw^*n^*(\sigma n^* + 2)}{(d_2\lambda_i - b)(1 + \sigma n^* + n^{*2}) + w^*n^*(\sigma n^* + 2)} > p.$$

Since $R(L) = (\ker L^*)^\perp$,

$$\text{codim}R(L(d_{1,i})) = \dim\ker L^*(d_{1,i}) = 1.$$

Finally, owing to

$$F_{d_1Q}(d_{1,i}, (0,0))\Phi_i = \begin{pmatrix} \Delta & 0 \\ 0 & 0 \end{pmatrix}\Phi_i = \begin{pmatrix} -\lambda_i\phi_i \\ 0 \end{pmatrix},$$

and

$$\langle F_{d_1Q}(d_{1,i}, (0,0))\Phi_i, \Phi_i^*\rangle = -\lambda_i \int_0^\pi \phi_i^2 dx = -\lambda_i \neq 0, \tag{B.1}$$

we obtain $F_{d_1Q}(d_{1,i}, (0,0))\Phi_i \notin R(L(d_{1,i}))$, and the proof for the simple eigenvalue is completed. □

C. Inapplicability of the Crandall-Rabinowitz bifurcation theory under double eigenvalues

Rewrite the map $F : R^+ \times X \to Y$, In the following form:

$$\begin{aligned} F(d_1, Q) &= \begin{pmatrix} d_1w'' + a - (w + w^*) - \dfrac{(w + w^*)(n + n^*)^2}{\sigma(n + n^*) + (n + n^*)^2 + 1} \\ d_2n'' + \dfrac{p(w + w^*)(n + n^*)^2}{\sigma(n + n^*) + (n + n^*)^2 + 1} - b(n + n^*) \end{pmatrix} \\ &= L(d_1)\begin{pmatrix} w \\ n \end{pmatrix} + \begin{pmatrix} F^1(w, n) \\ F^2(w, n) \end{pmatrix}, \end{aligned} \tag{C.1}$$

where $F^1(w, n) = -pF^2(w, n)$ and

$$\begin{aligned} F^2(w^*, n^*) = &\frac{n^*(2 + \sigma n^*)}{(1 + \sigma n^* + n^{*2})^2}w^*n^* + \frac{1 + \sigma n^* - 2n^{*2} - 4\sigma n^{*3} - \sigma^2 n^{*4}}{n^*(1 + \sigma n^* + n^{*2})^3}n^{*2} \\ &+ \frac{1 + \sigma n^* - 2n^{*2} - 4\sigma n^{*3} - \sigma^2 n^{*4}}{(1 + \sigma n^* + n^{*2})^4}w^*n^{*2} + O(|n^3|, |n^3||w|). \end{aligned} \tag{C.2}$$

Then, suppose there exists a positive integer $i(\neq j)$ such that $d_{1,i} = d_{1,j} = \hat{d}_1$.

Let $L(\hat{d}_1) = F_Q(\hat{d}_1, (0,0))$. Consequently, we obtain

$$\ker L(\hat{d}_1) = \text{span}\{\Phi_i, \Phi_j\}, \quad \ker L^*(\hat{d}_1) = \text{span}\{\Phi_i^*, \Phi_j^*\}$$

and

$$M(L(\hat{d}_1)) = \{(w, n)^T \in Y : \int_0^\pi (w + e_i^*n)\phi_i dx = \int_0^\pi (w + e_j^*n)\phi_j dx = 0\}.$$

It follows that

$$\dim\ker L(\hat{d}_1) = \text{codim}M(L(\hat{d}_1)) = 2.$$